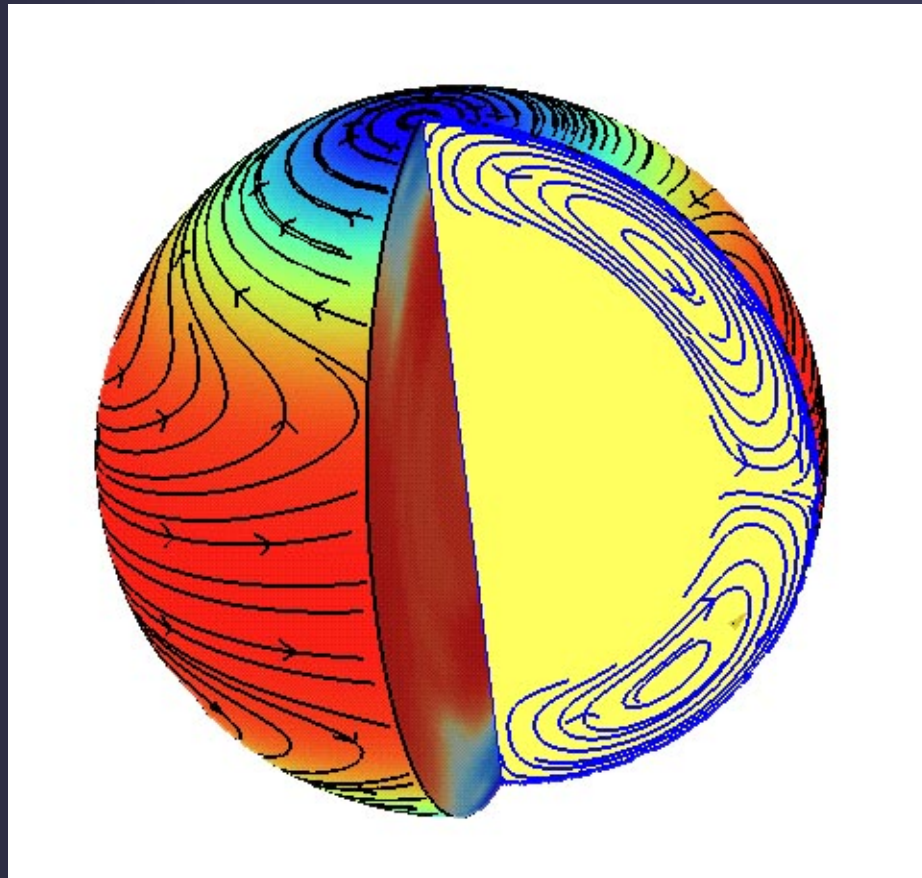


Solar rotation



Solar rotation

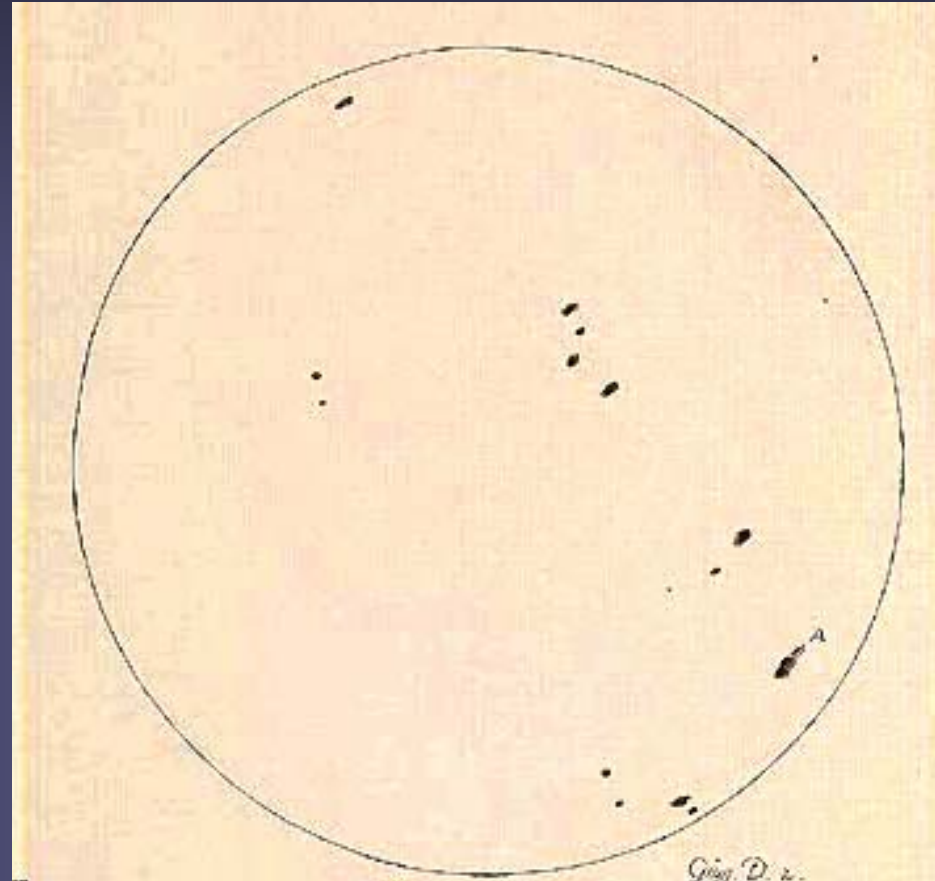
- The Sun rotates differentially, both in latitude (equator faster than poles) and in depth (strong shear at bottom of convection zone).
- Standard value of solar rotation: Carrington rotation period: 27.2753 days (the time taken for the solar coordinate system to complete one rotation as seen from Earth).
- Sun's rotation axis is inclined by 7.1° relative to the Earth's orbital axis (i.e. the Sun's equator is inclined by 7.1° relative to the ecliptic).

Sidereal and synodic rotation

- Synodic rotation period = rotation period as seen from Earth. I.e. the period of time it takes for a feature on the Sun to return to the same position as seen from Earth.
 - the Standard synodic rotation period is the Carrington period of 27.2753 days
- Sidereal rotation period = rotation period relative to the stars
 - The sidereal rotation period corresponding to the Carrington period is: 25.38 days
- Difference between the two is due to the rotation of the Earth around the Sun.

Discovery of solar rotation

- Galileo Galilei and Christoph Scheiner noticed already that sunspots move across the solar disk in accordance with the rotation of a round body
- Sun is a rotating sphere
- Movie based on Galileo Galilei's historical data



Surface differential rotation

- Poles rotate more slowly than equator.
- Surface differential rotation from measurements of:
 - Tracers: sunspots or magnetic field elements (these indicate the rotation rate of magnetic field)
 - Coronal holes (not plotted) rotate rigidly
 - Doppler shifts of the gas

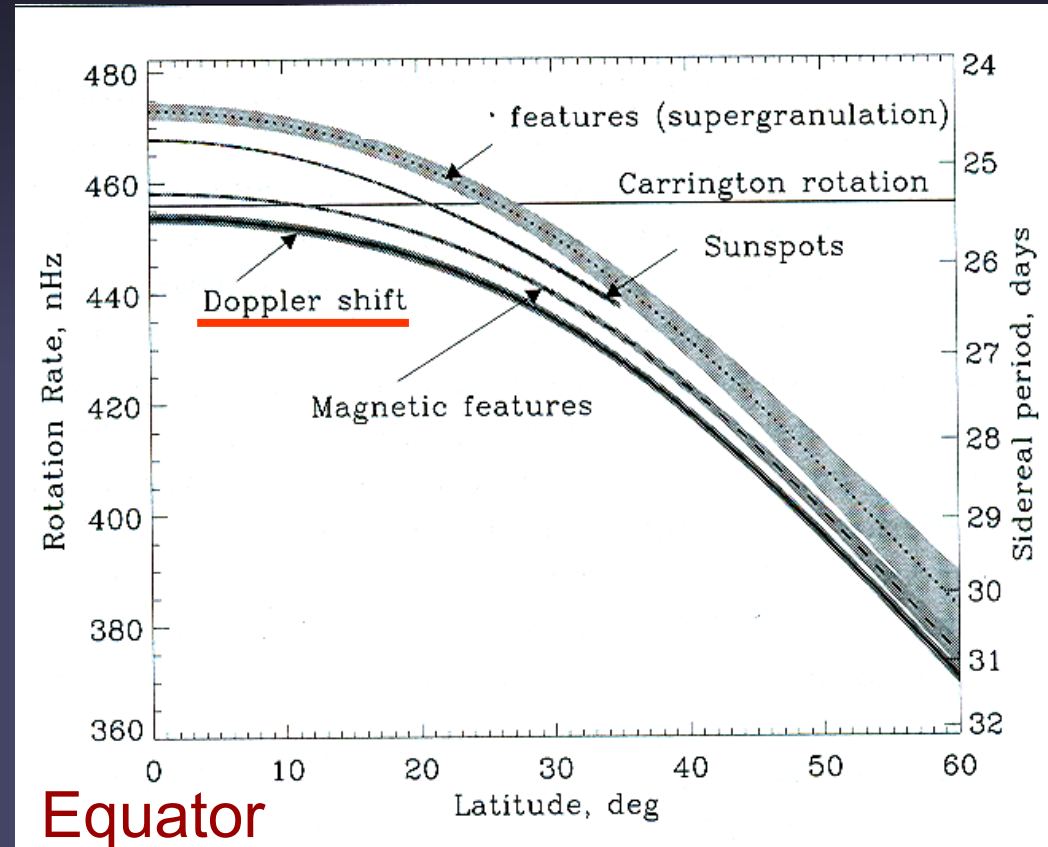


Figure 1. Rotation rate, $\Omega/2\pi$, and period of various tracers on the Sun's surface: recurrent (old) sunspots (dashed curve), magnetic features (dot-dash), and Doppler features (dots). The rotation rate and period determined spectroscopically through the Doppler shift are shown by the full curve. The shaded areas show the 1σ error estimates.

Surface differential rotation

- Description:

$$\Omega = A + B \sin^2\psi + C \sin^4\psi$$

where ψ is the latitude, $A = \Omega$ at the equator and $A+B+C = \Omega$ at the poles.

- Different tracers give different A , B , C values. E.g. spots rotate faster than the surface gas.

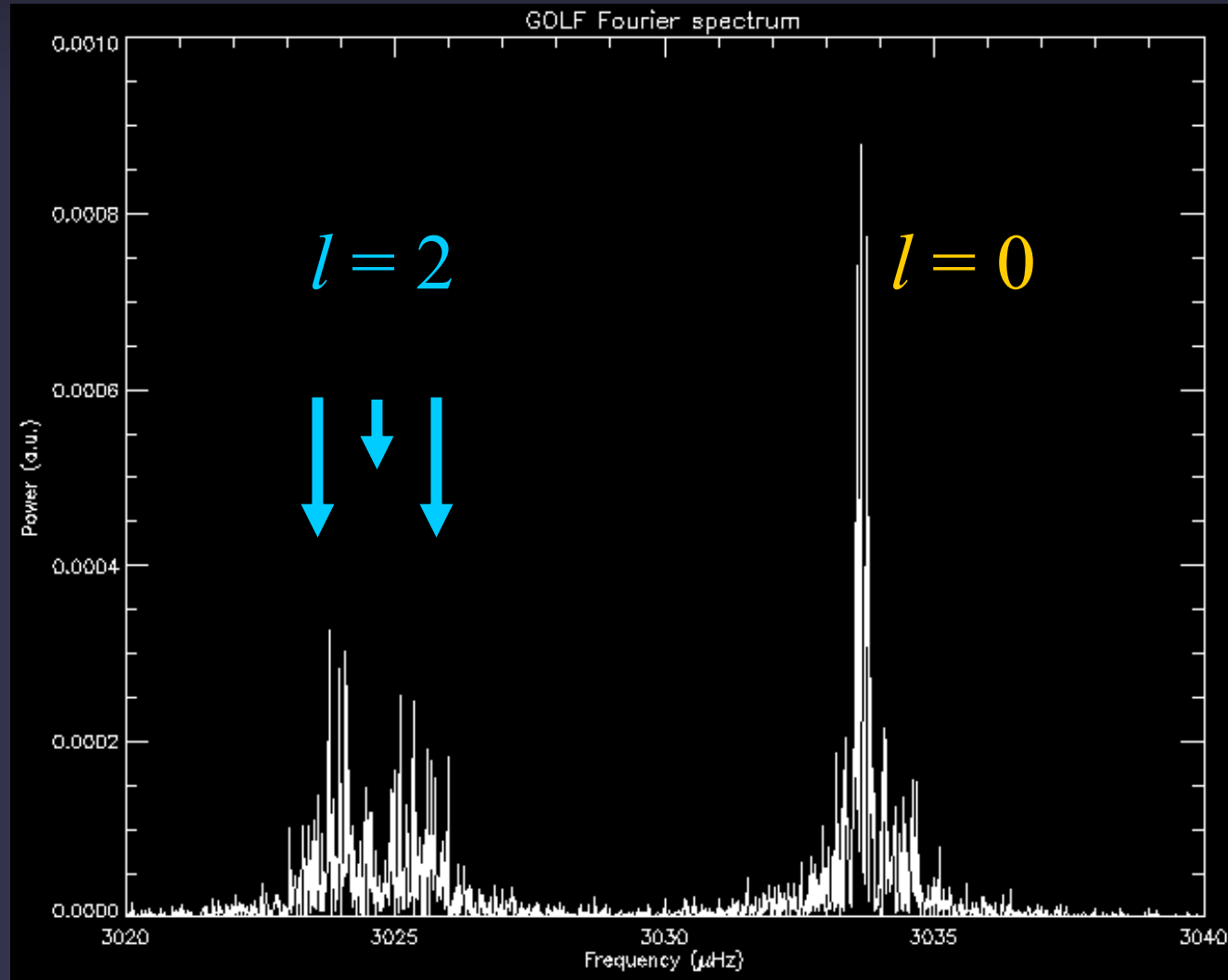
Internal differential rotation

■ Method: Helioseismic inversions

- In a non-rotating star the individual modes of oscillation, described by “quantum numbers” n, l, m are degenerate in that their frequency depends only on n and l , but not on m .
- Similar to Zeeman effect. Note that m distinguishes between the surface distribution of oscillation nodes. For a spherically symmetric star (no rotation) all these modes must have same frequency.
- In a rotating Sun the degeneracy is removed and modes with different m have slightly different frequency.
- Since modes with different l sample the solar latitudes in different ways, it is possible to determine not just vertical, but also latitudinal differential rotation by helioseismology.

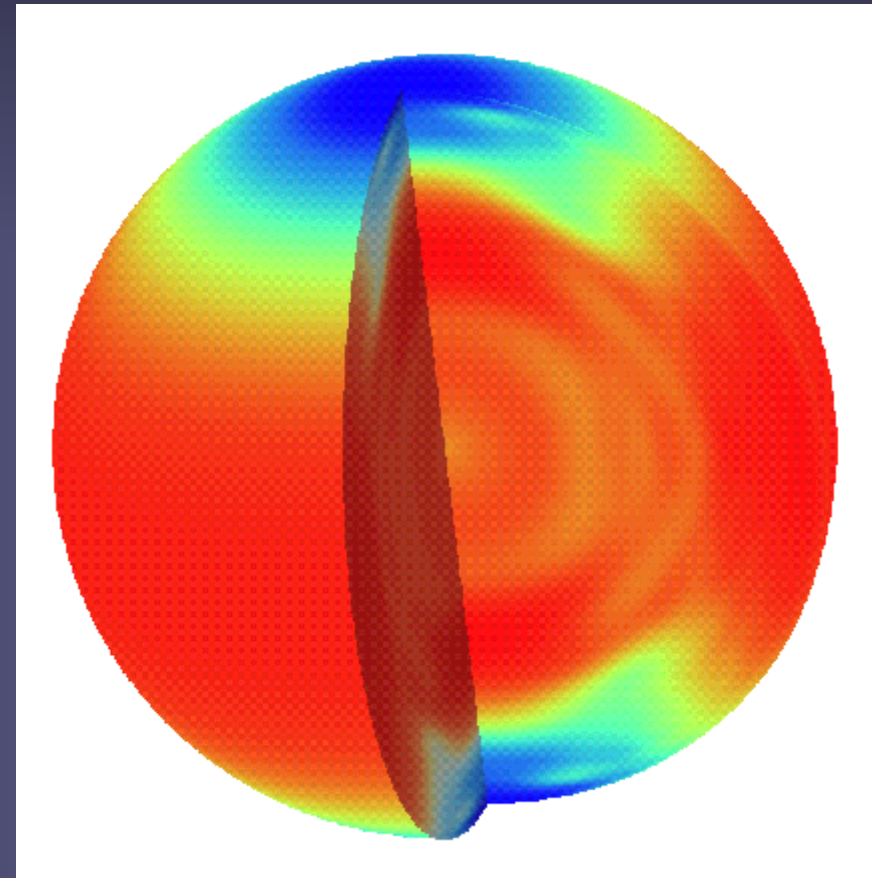
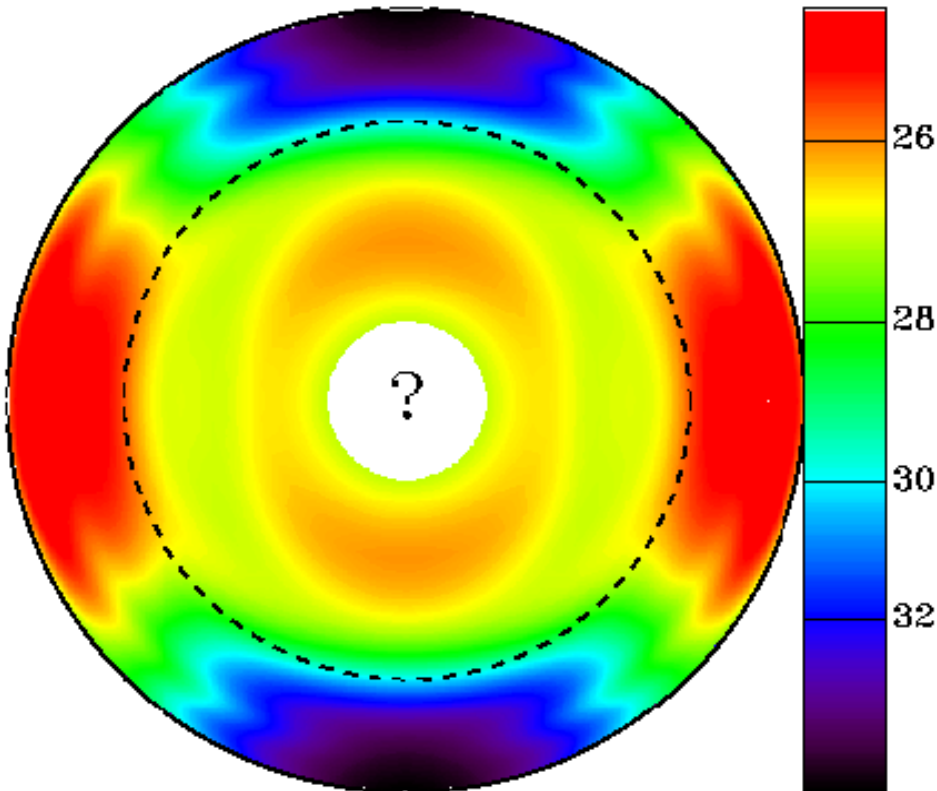
Mode structure: Rotational splitting

- GOLF/SOHO observations showing a blowup of the power spectrum with an $l=0$ and an $l=2$ mode.
- The noise is re-excitation noise
- The extra width of the $l=2$ mode is due to solar rotation splitting



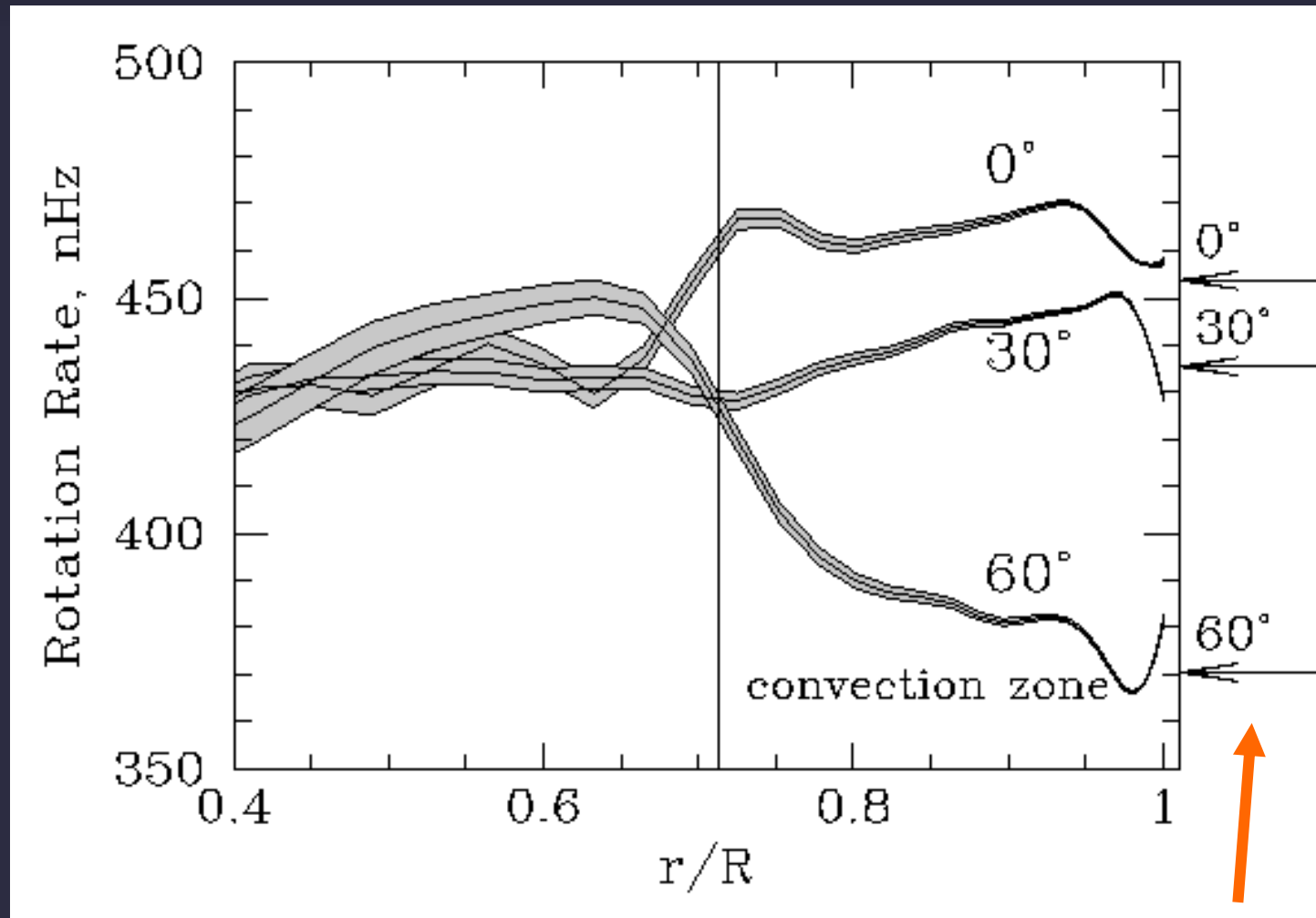
Internal differential rotation II

- Structure of internal rotation deduced from MDI data
- Note: differential rotation in CZ, solid rotation below



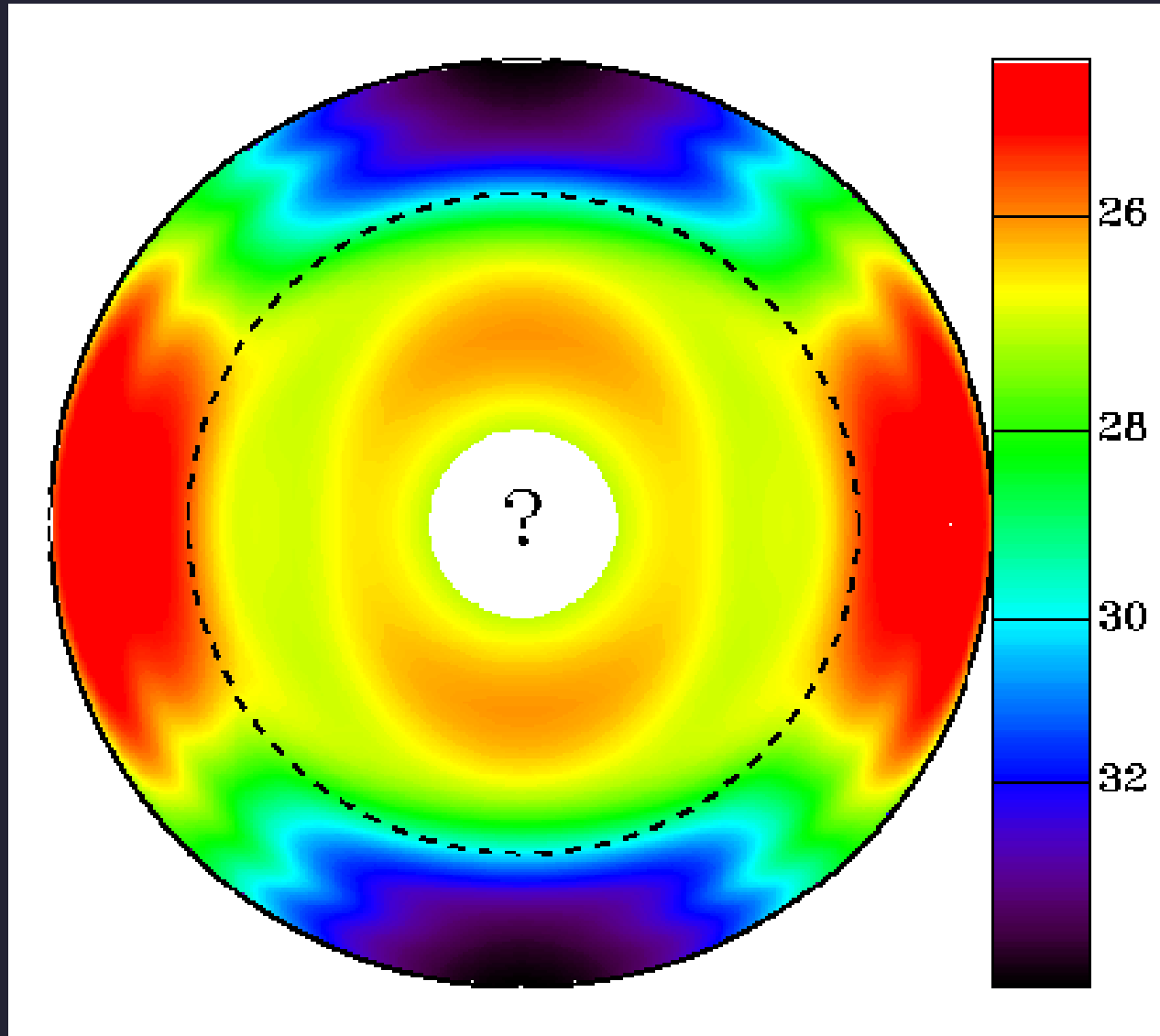
Internal differential rotation III : tachocline

Large radial gradients in rotation rate at bottom of CZ (tachocline), but also just below solar surface (enigmatic). Note the slight mismatch of helioseismic and Doppler measurements



Doppler measurements

What about rotation of solar core?



What about rotation of solar core?

- Rotation rate of solar core is hard to determine, since p-modes do not penetrate to the Sun's centre.
- Different values in the literature for the core's rotation rate: $\Omega(r=0) = \Omega(r=R_{\odot}) \dots 2 \Omega(r=R_{\odot})$
- One way to set limits on $\Omega(r=0)$: quadrupole moment of Sun.
- Solar rotation leads to oblateness, i.e. diameter is larger at equator than between the poles.
- If core rotates more rapidly than surface, then oblateness will be larger than expected due to surface rotation rate.

Solar oblateness

- Oblateness = $\Delta R/R_{\odot}$
- Direct measurements: $\Delta R/R_{\odot} \approx 10^{-5}$
 - Very tricky, since oblateness 10^{-5} corresponds to $\Delta R = 14$ km (best spatial resolution achievable: 100 km).
 - Systematic errors due to concentration of magnetic activity to low latitudes \rightarrow affects measurements of solar diameter, since shape of limb is distorted.
 - Initial measurements due to Dicke & Goldenberg (1967) gave $\Delta R/R_{\odot} \approx 5 \times 10^{-5} \rightarrow$ required change of general relativity to explain motion of Mercury's perihelion (but was consistent with Brans-Dicke gravitation theory)
- Helioseismic measurements give for the acoustic radius of the Sun (which is not the same as the optical radius, but similar): $\Delta R/R_{\odot} \approx 10^{-5}$

Evolution of solar rotation

- Young stars are seen to rotate up to 100 times faster than the Sun.
- Did the Sun also rotate faster when it was young?
- Skumanich law: $\Omega \sim t^{-1/2}$, where t is the age of the star (deduced from observing stars in clusters of different ages). I.e. old cool stars also rotate slowly.
- Sun also rotated faster as a young star.
- Question: where did all the angular momentum go?

Evolution of solar rotation II

- Question: where did all the angular momentum go?
- Answer part 1: Solar wind! The solar wind carries away angular momentum with it. Torque j , i.e. rate of change of angular momentum, exerted by solar wind (without magnetic field):

$$j = \Omega R_{\odot} dm/dt$$

- Here dm/dt is the solar mass-loss rate (mass carried away by solar wind)
- Problem: j is 2-3 orders of magnitude too small to cause a significant braking of solar rotation...

Evolution of solar rotation III

- Answer part 2: Magnetic field!
- Below Alfvén radius R_A , i.e. point where wind speed becomes $>$ Alfvén speed, wind is channeled by the field. Up to that radius, the wind rotates rigidly with the solar surface (forced to do so by rigid field lines), i.e. wind carries angular momentum away only beyond R_A . It is as if the Sun had the radius R_A .
Proper expression for Torque:

$$j = \Omega R_A dm/dt$$

- R_A typically is 10-20 times larger than R_\odot for today's Sun.

Evolution of rotation IV

- $j = \Omega R_A dm/dt \sim \Omega$

→ The faster the star rotates, the quicker it spins down.

- Additional corrections:

- dm/dt depends on Ω (more rapidly rotating star, more magnetic field, hotter the corona, larger the dm/dt)

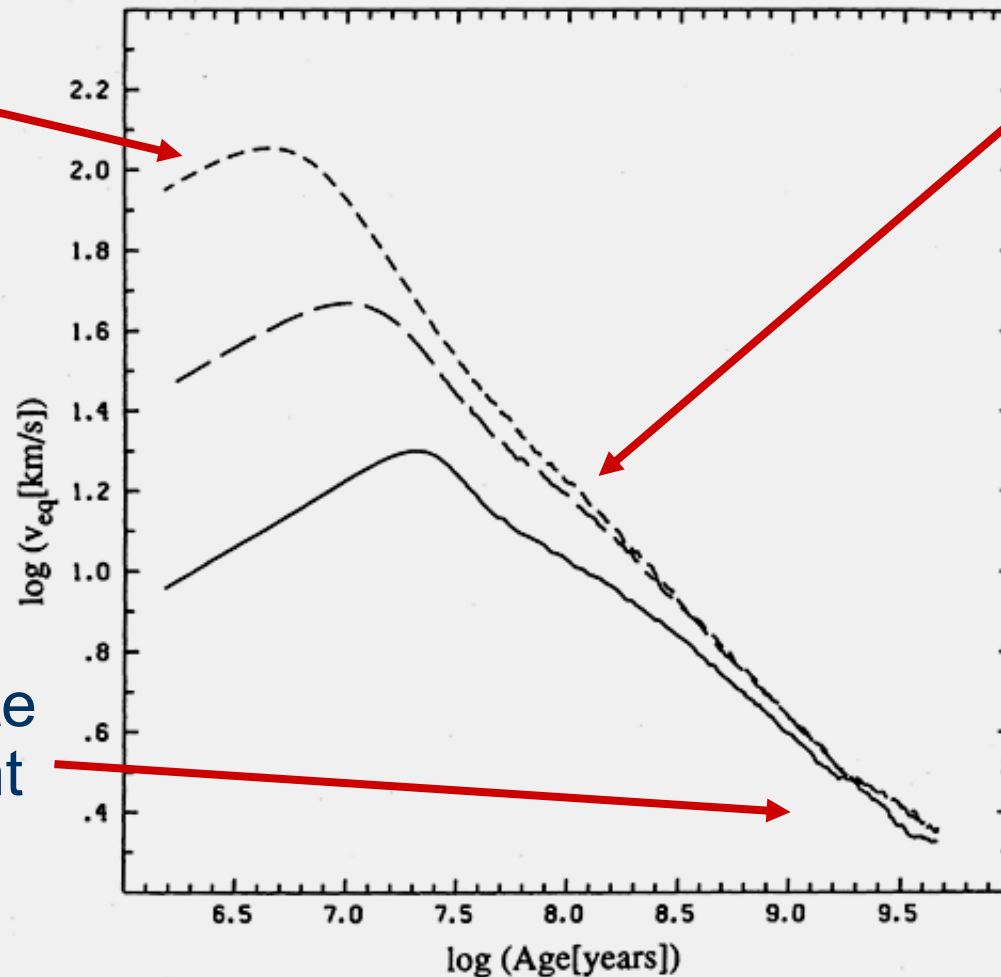
- R_A depends on Ω (although not in a straightforward manner: more rapidly rotating star, more magnetic field, but also larger the density and velocity of wind).

- In general $j = k\Omega^\alpha$, where α typically > 1 , although there are signs that for very large Ω , the α value becomes very small (saturation).

Solar rotation velocity evolution

Spinup
as the
star
contracts
towards
the main
sequence

Current
Rotation rate
independent
of starting
value



Spindown
due to
magnetic
braking
(wind loss)

Pinsonnault
et al.

FIG. 3.—Surface rotation velocity as a function of time for three models differing only in initial angular momentum. The solid line is the reference solar model (case A in Table 2) with $J_0 = 5 \times 10^{49} \text{ g cm}^2 \text{ s}^{-1}$. The long-dashed line is a model with $J_0 = 1.63 \times 10^{50} \text{ g cm}^2 \text{ s}^{-1}$ (case B). The short-dashed line is a model with $J_0 = 5 \times 10^{50} \text{ g cm}^2 \text{ s}^{-1}$ (case C). An order of magnitude in J_0 produces only a small variation in the surface rotation velocity on the main sequence ($\log t > 8$).

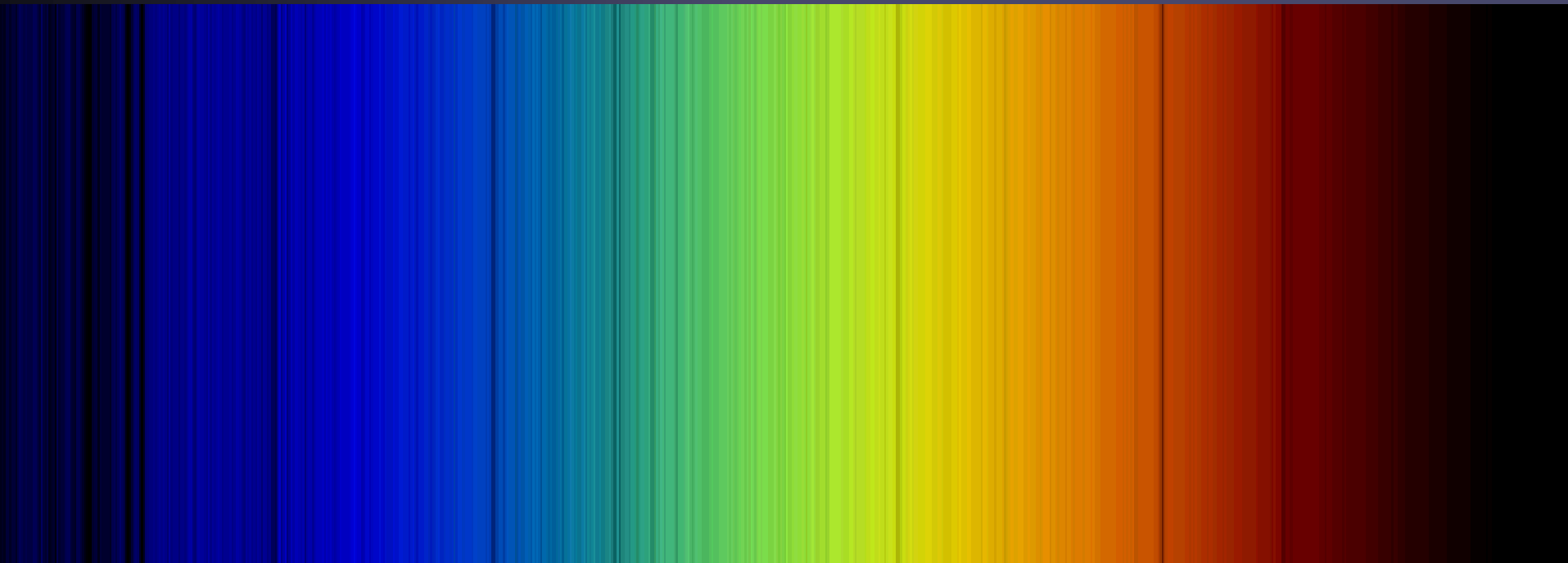
Complexity

- Solar physics is a complex field, requiring a lot of teamwork.

→ Finagle's rule:

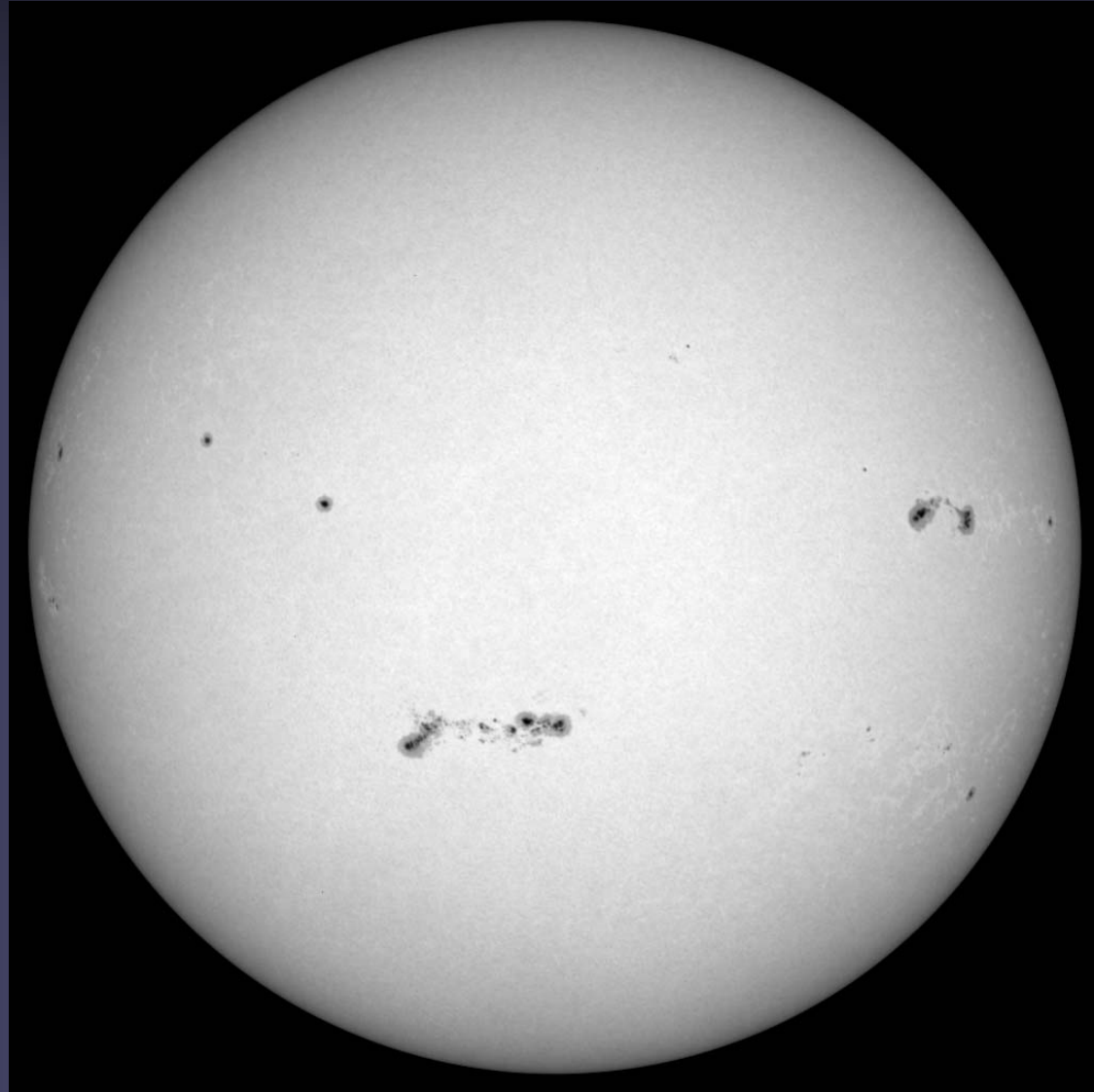
Teamwork is essential. It allows you to blame someone else when things go wrong.

Solar radiation and spectrum



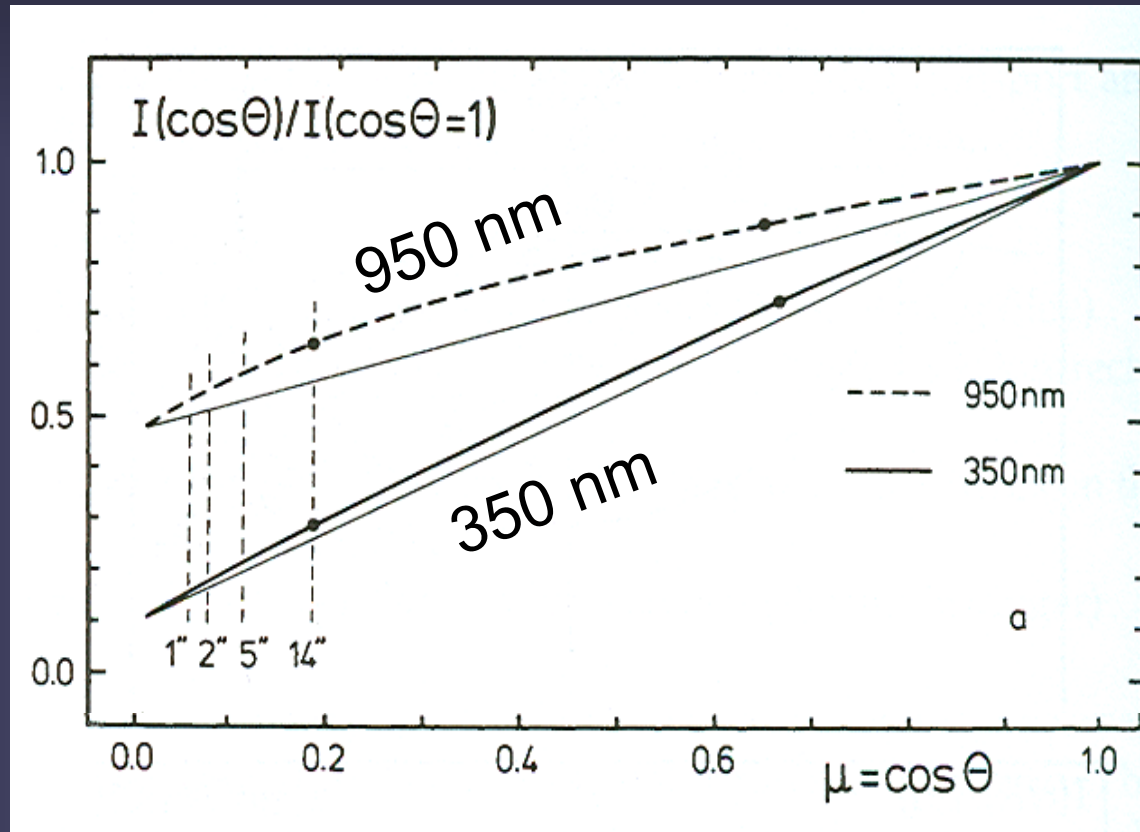
The Sun in white light: Limb darkening

- In the visible, Sun's limb is darker than solar disc centre (→ limb darkening)
- Since intensity \sim Planck function, $B_\nu(T)$, T is lower near limb.
- Due to grazing incidence we see higher near limb: T decreases outward



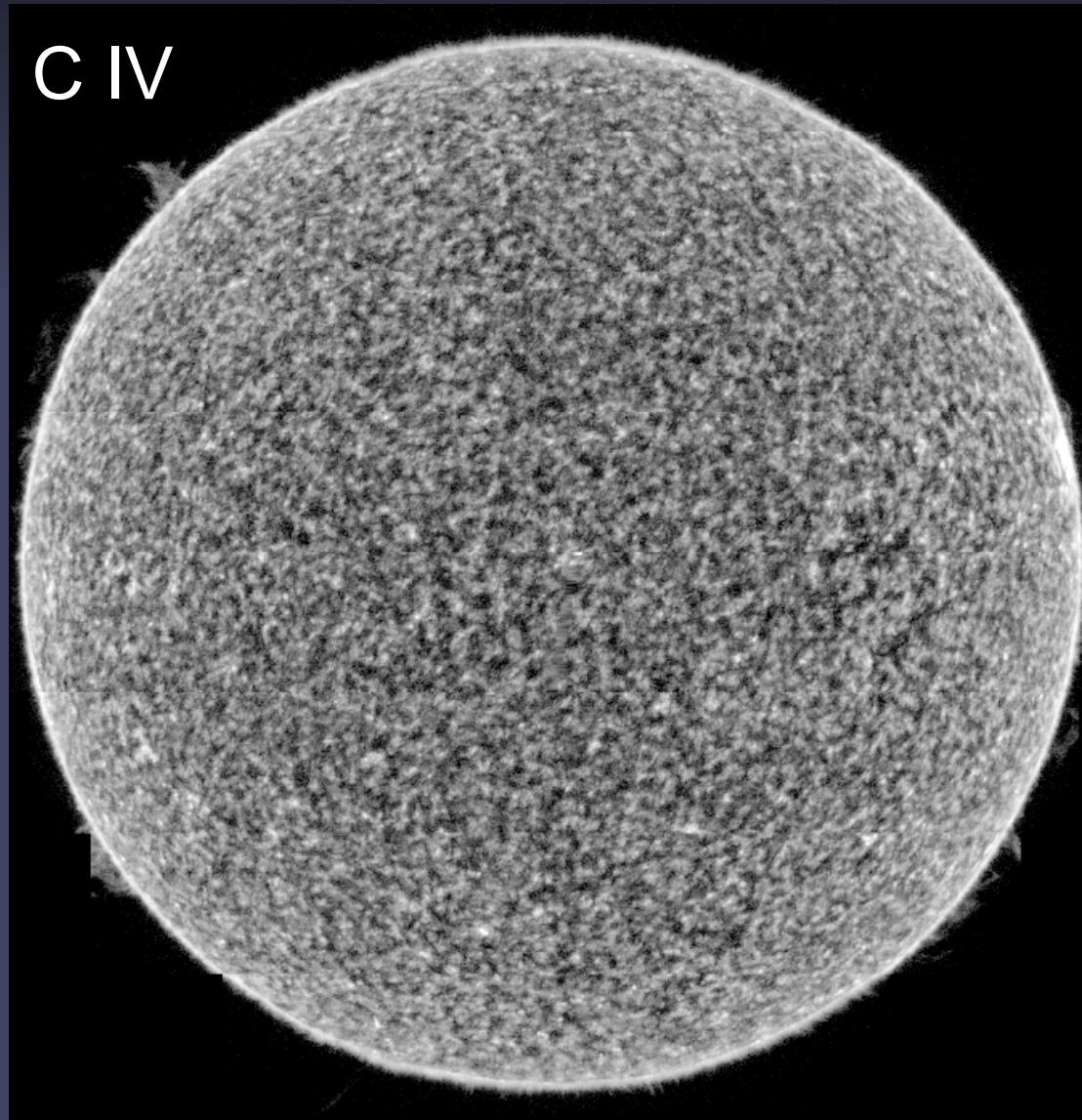
Limb darkening vs. λ

- short λ : large limb darkening;
- long λ : small limb darkening
- departure from straight line: limb darkening is more complex than $I(\theta) \sim \cos(\theta)$



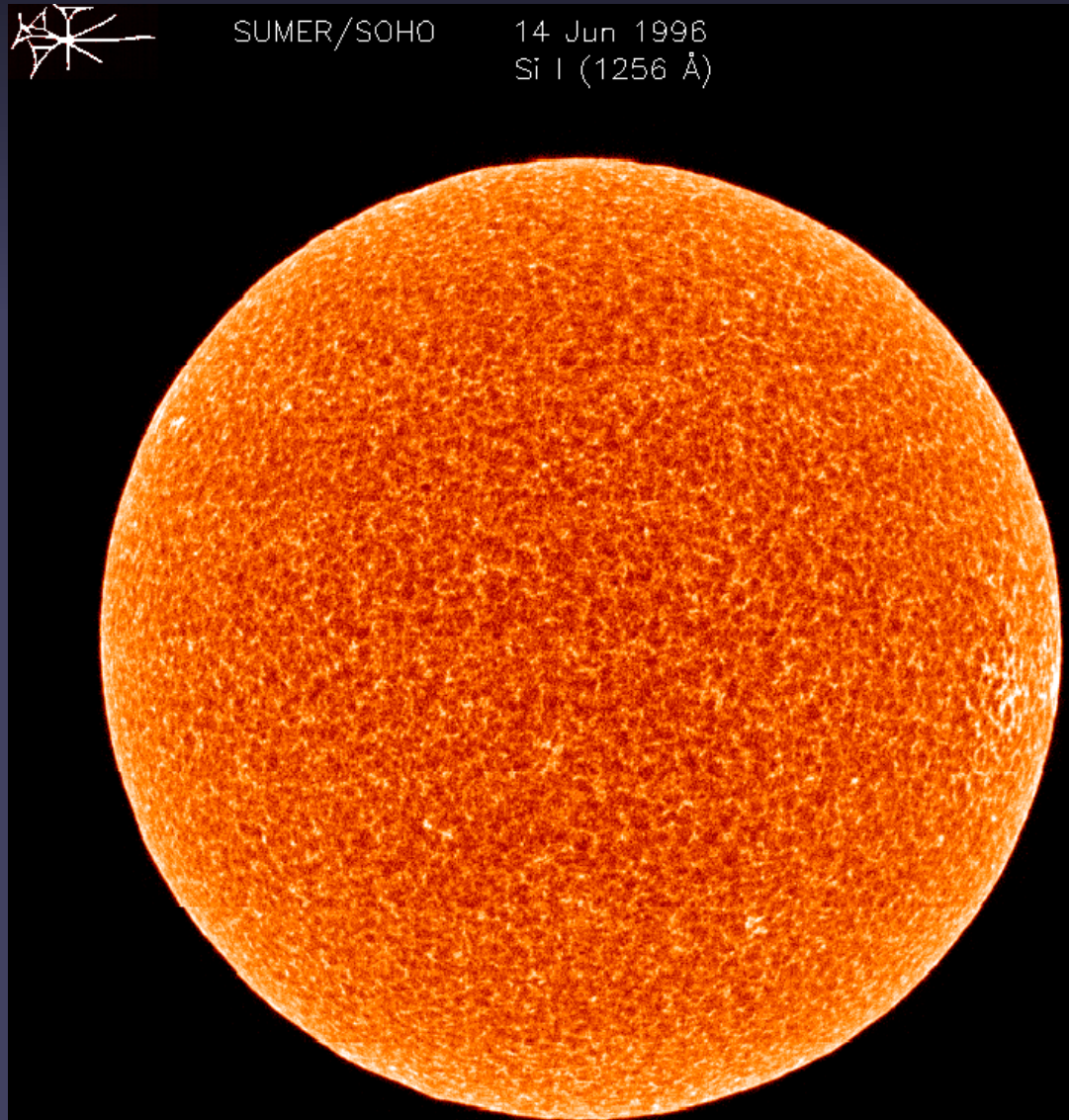
The Sun in the EUV: Limb brightening

- In the EUV, Sun's limb is brighter than disc centre (→ limb brightening)
- Solar atmosphere is optically thin at EUV wavelengths → intensity \sim thickness of layer contributing to it. Near the limb this layer appears thicker (optically thin radiation comes from roughly the same height everywhere).



The Sun in the EUV: Limb brightening

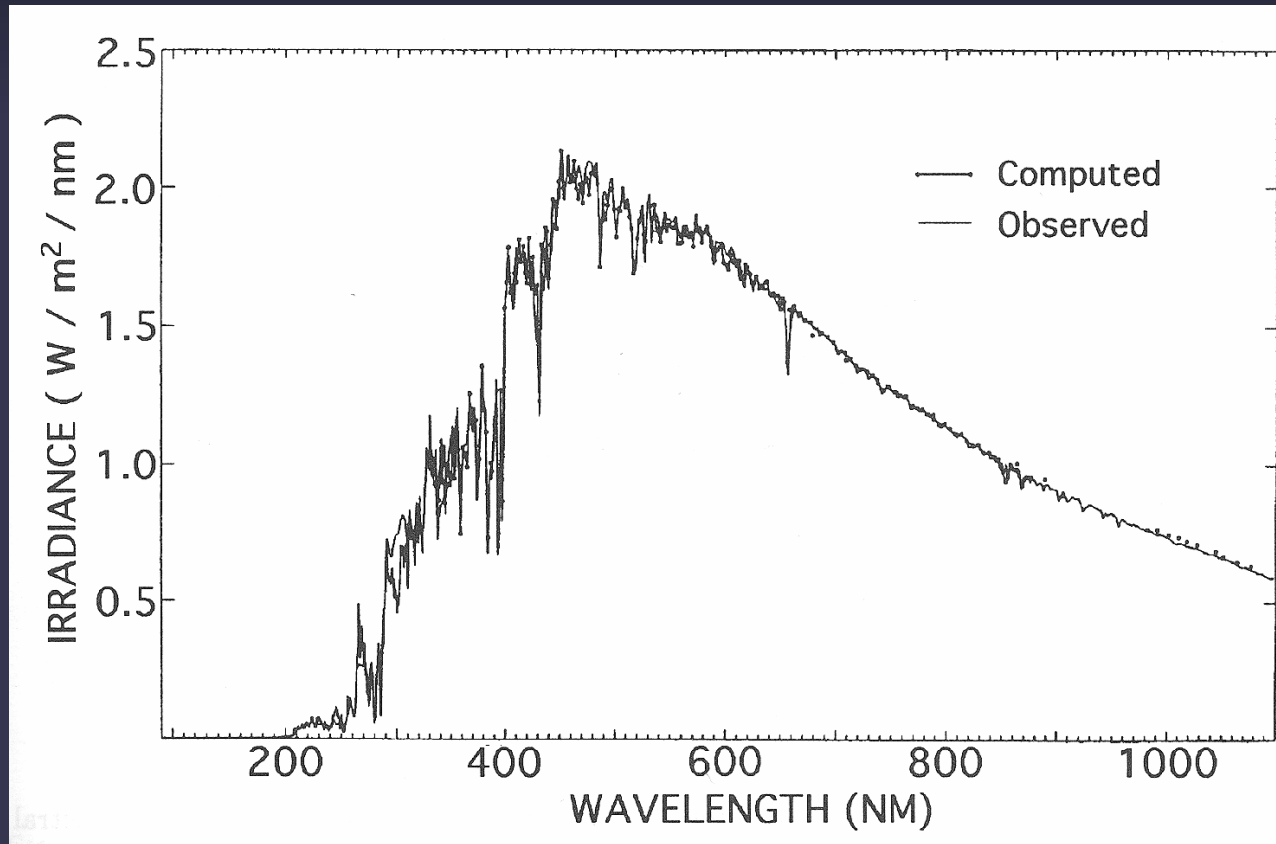
- Limb brightening in optically thin lines does NOT imply that temperature increases outwards (although by chance it does in these layers....)



Solar irradiance spectrum

Irradiance = solar flux at 1AU

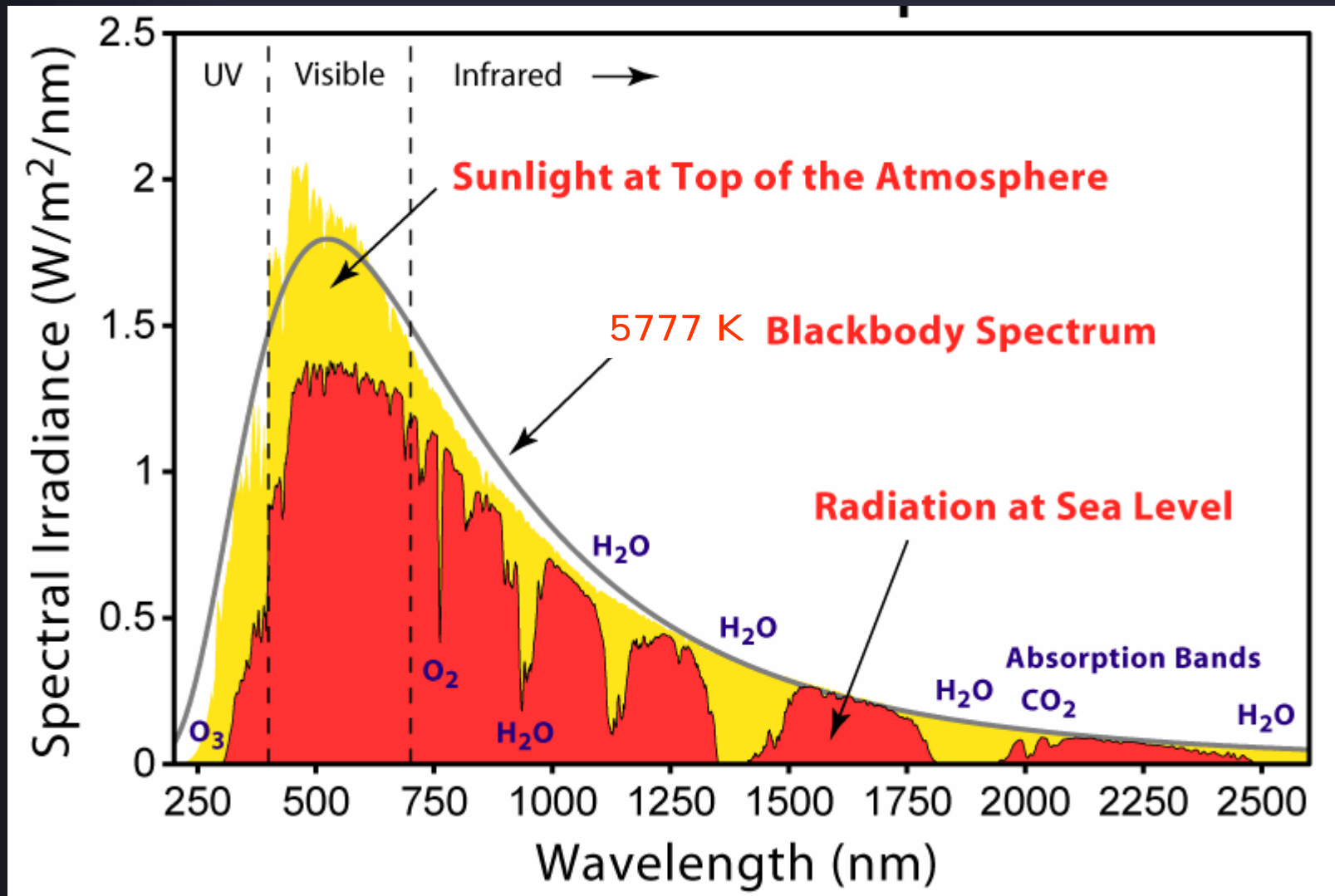
Spectrum is similar to, but not equal to Planck function
→ Radiation comes from layers with diff. temperatures.



Often used temperature measure for stars:

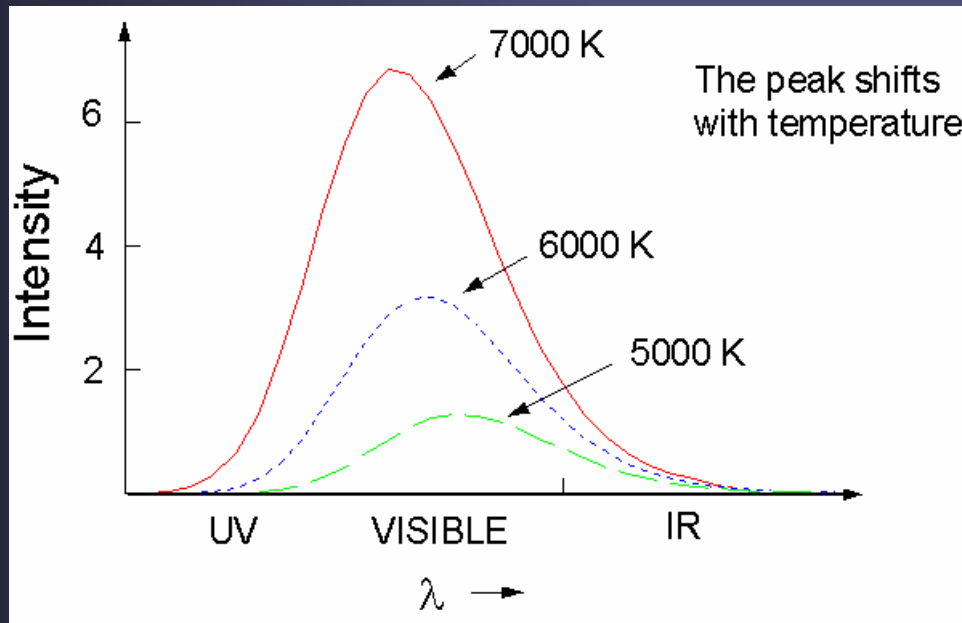
Effective temp: $\sigma T_{\text{eff}}^4 = \text{Area under flux curve}$

Spectrum above and under the Earth's atmosphere



Planck's function

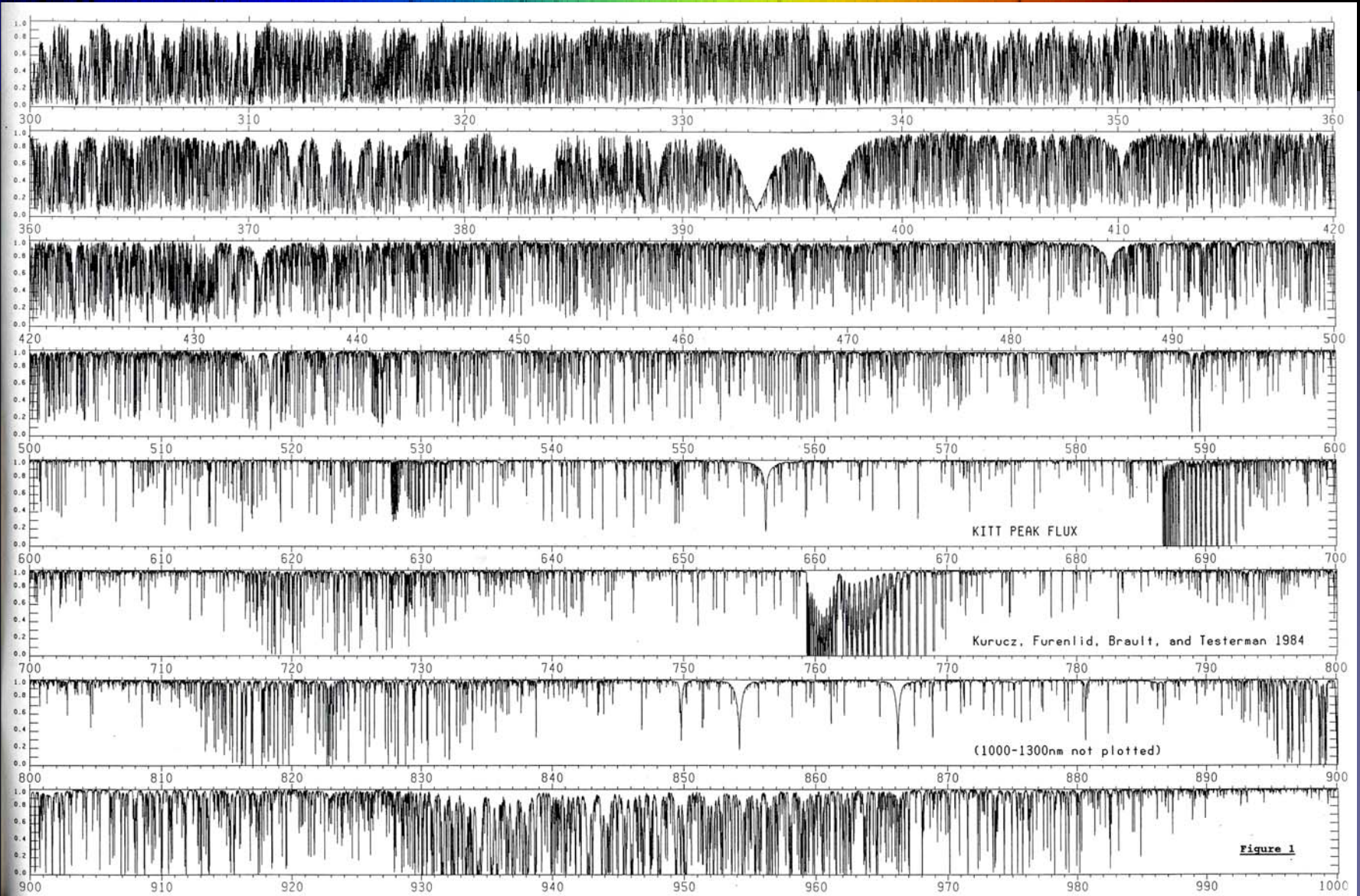
- Amplitude and area increases approximately exponentially with temperature \rightarrow from e.g. λ -integrated intensity we get effective temperature
- Wavelength of maximum changes linearly with temperature (Wien's law)



The solar spectrum: continua with absorption and emission lines

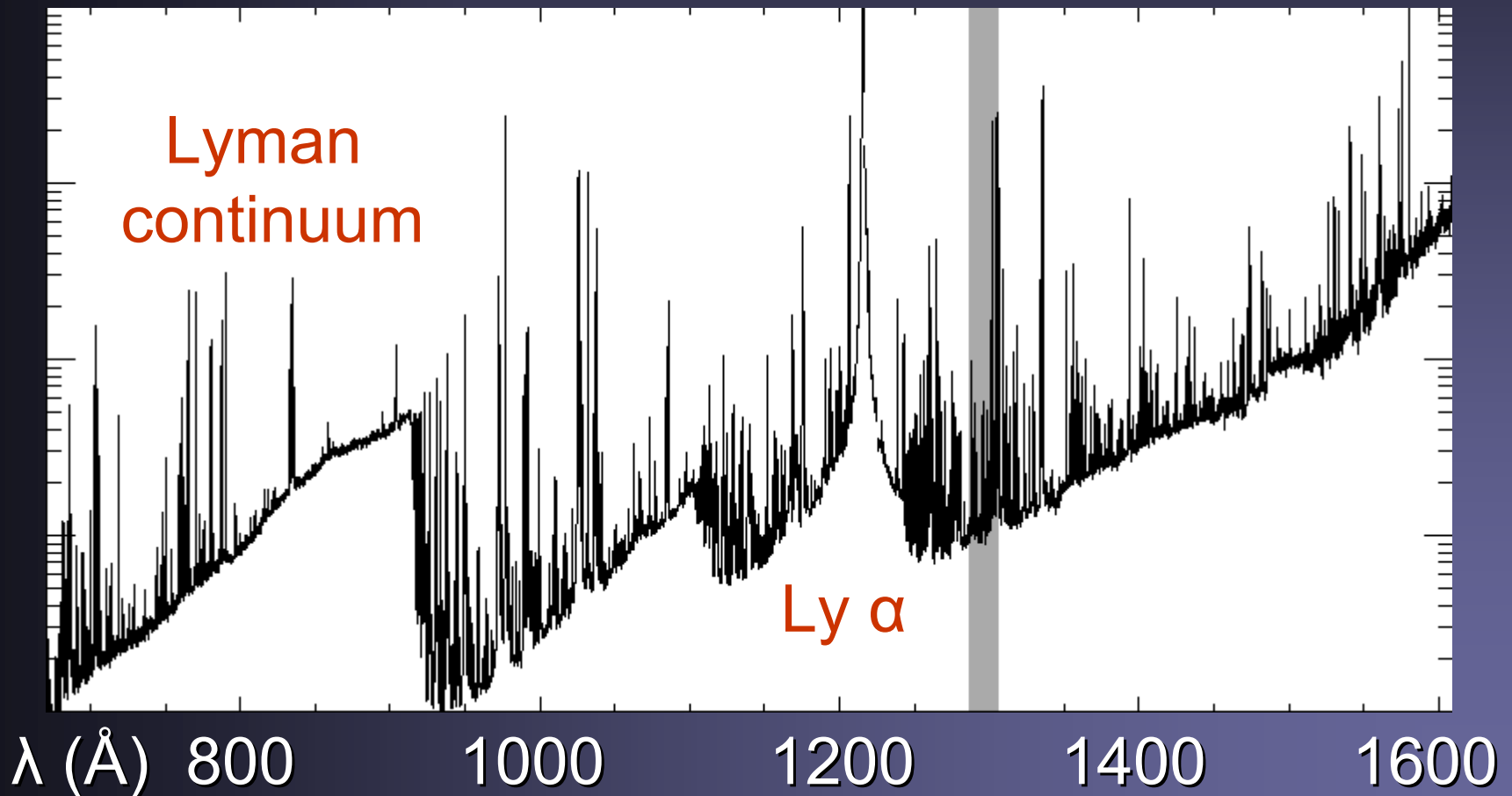
- Solar spectrum changes in character at different λ
- **X-rays**: Emission lines of highly ionized species
- **EUV**: Emission lines of neutral to multiply ionized species plus recombination continua
- **UV**: stronger recombination continua and absorption lines
- **Visible**: H^- b-f continuum with absorption lines
- **FIR**: H^- f-f continuum, increasingly cleaner (i.e. less lines, except molecular bands)
- **Radio**: thermal and, at longer λ , increasingly non-thermal continua

Visible

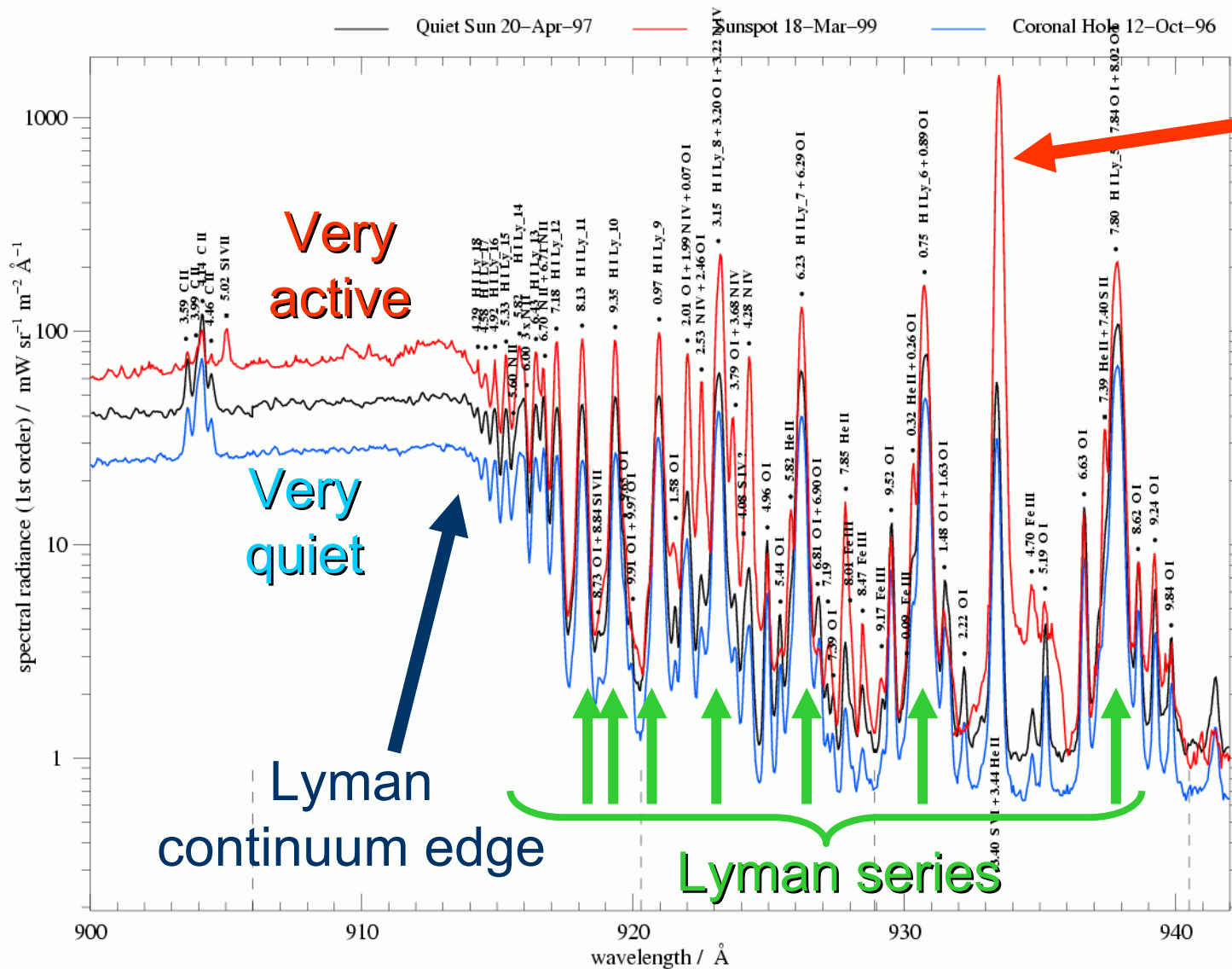


EUV spectrum

The solar spectrum from 670 Å to 1620 Å measured by SUMER (logarithmic scale)



Detail of EUV spectrum by SUMER



Activity sensitive line: S VI

Radiative transfer: optical depth

- Axis z points in the direction of light propagation
- Optical depth: $\Delta\tau_\nu = -\kappa_\nu \Delta z$,

where κ_ν is the absorption coefficient [cm^{-1}] and ν is the frequency of the radiation. Light only knows about the τ_ν scale and is unaware of z

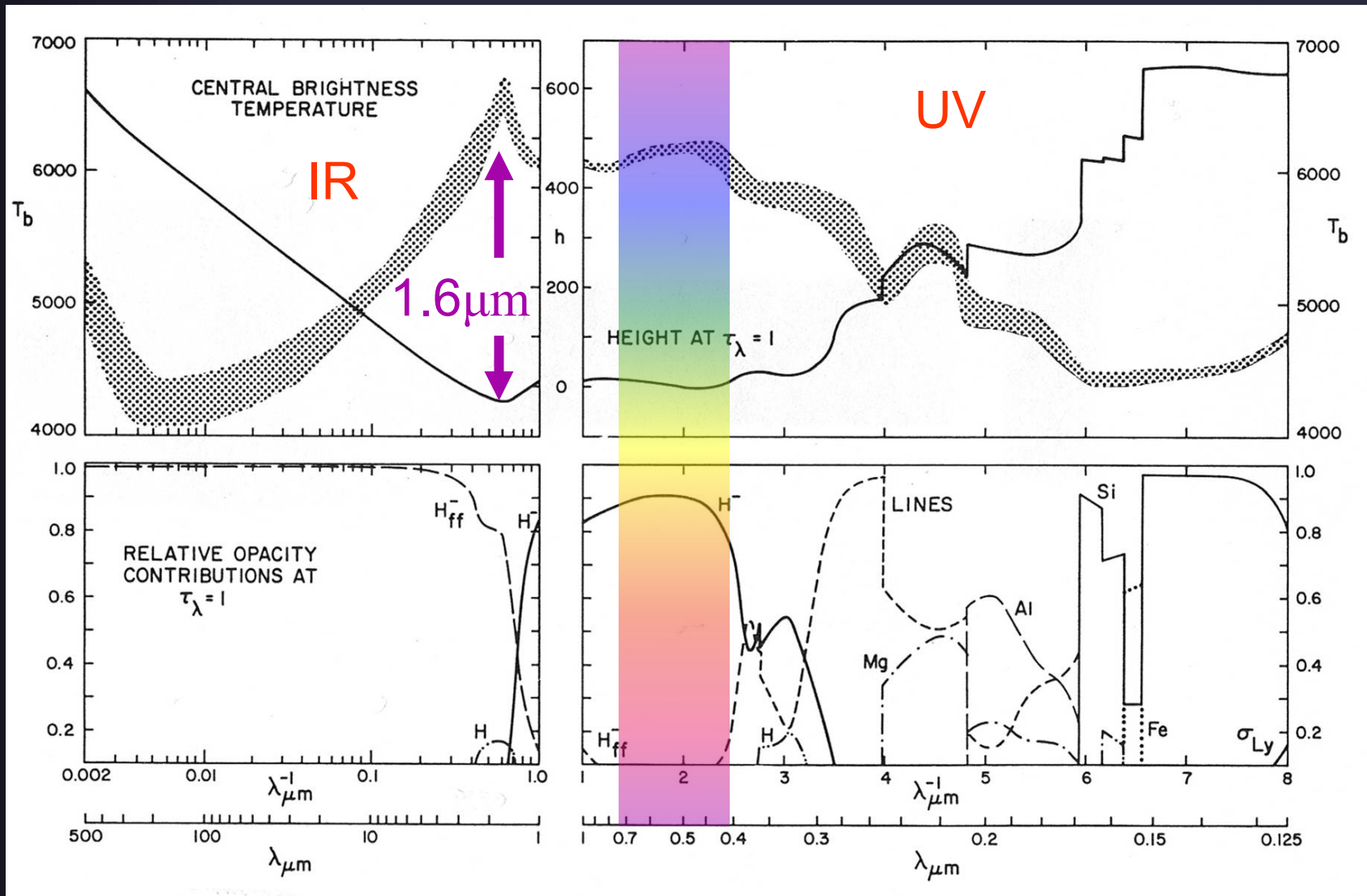
→ Integration over z : $\tau_\nu = -\int \kappa_\nu(z) dz$

(note that the scales are floating, no constant of integration is fixed)

Optical depth and solar surface

- Radiation at frequency ν escaping from the Sun is emitted mainly at heights around $\tau_\nu \approx 1$.
- At wavelengths at which κ_ν is larger, the radiation comes from higher layers in the atmosphere.
- In solar atmosphere κ_ν is small in visible and near IR, but large in UV and FIR \rightarrow We see deepest in visible and NIR, but sample higher layers at shorter and longer wavelengths.

Height of $\tau = 1$, brightness temperature and opacity vs. λ



Radiative Transfer Equation

- Equation of radiative transfer:

$$\mu \, dI_\nu / d\tau_\nu = I_\nu - S_\nu$$

where I_ν is the intensity (i.e. the measured quantity) and S_ν is the source function. $\mu = \cos\theta$, where $\theta =$ angle of line-of-sight to surface normal.

- $S_\nu =$ emissivity ϵ_ν divided by absorption coefficient κ_ν
- The physics is hidden in ϵ_ν and κ_ν , i.e. in τ_ν and S_ν .
- These quantities depend on temperature, pressure, elemental abundances and frequency (or wavelength)

Formal solution of RT equation

- For $S_\nu = 0$ the solution of the RTE in a slab with (optical) boundaries $\tau_{\nu 2}$ and $\tau_{\nu 1}$ is ($\tau_{\nu 2} > \tau_{\nu 1}$):

$$I_\nu(\tau_{\nu 1}) = I_\nu(\tau_{\nu 2}) \exp(-\tau_{\nu 2} + \tau_{\nu 1})$$

- For general case formal solution reads (formal soln. assumes that we already know S_ν)

$$I_\nu(\tau_{\nu 1}) = I_\nu(\tau_{\nu 2}) \exp(-\tau_{\nu 2} + \tau_{\nu 1}) + \int S_\nu \exp(-\tau_\nu) d\tau_\nu$$

- 1st term describes radiation that enters through lower boundary (only absorption, no emission in slab), 2nd term describes radiation emitted in slab.
- In a stellar atmosphere $\tau_{\nu 2} = \infty$, so that only the 2nd term survives (lower boundary is unimportant).

When is an emission line formed, when an absorption line?

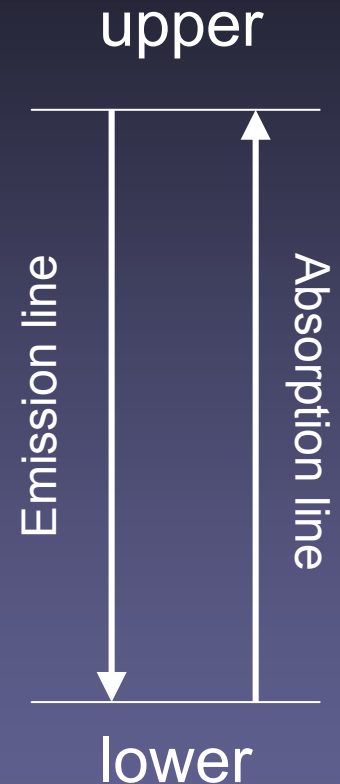
- Continua are formed deeper in a stellar atmosphere than spectral lines at the same wavelengths:

$$\kappa_L + \kappa_C > \kappa_C$$

- A line is in absorption if S_ν decreases with height, i.e. if the absorption at greater heights dominates over emission ($S_L < S_C$)
- A line is in emission if S_ν increases with height, i.e. if the emission at greater heights dominates over absorption ($S_L > S_C$)

Statistical equilibrium

- In general both S_ν and κ_ν require a computation of the full statistical equilibrium for the atomic species being considered.
- This implies computing how much each atomic/ionic/molecular level is populated, i.e. solving rate equations describing transitions to and from each considered level.
- Requires detailed knowledge of atomic, ionic, molecular structure and transitions.



The assumption of LTE

- In solar interior and photosphere (i.e. where density is large and collisions are common) we can assume **Local Thermodynamic Equilibrium (LTE)**
- Thermodynamic equilibrium (TE): a single temp. everywhere = blackbody → Emerging radiation follows Planck function $B_\nu(T)$.
- **LTE**: Each layer of the solar atmosphere has its own temperature → Replace S_ν by $B_\nu(\tau, T)$ in the RTE and its solution.
 - Problem of knowing S_ν is reduced to knowing $T(\tau)$ in the atmosphere.
 - equilibrium reduces to Saha-Boltzmann equilibrium → Only T and n_e need to be known.

Saha and Boltzmann equations

Excitation (Boltzmann) and ionization (SAHA) in LTE

$$\frac{n_{low}}{n_{up}} = \frac{g_{low}}{g_{up}} e^{-(E_{low} - E_{up}) / kT}$$

Boltzmann

n = number density of particles in a particular energy state
 g = statistical weight of level: $g = 2J + 1$, J = angular momentum
 E = Energy of levels involved in the transition

$$\frac{n_{up}}{n_{low}} = \frac{2}{n_e} \left(\frac{2\pi m_e kT}{h^3} \right)^{3/2} \frac{g_{up}}{g_{low}} e^{-(E_{up} - E_{low}) / kT}$$

Saha

n_e = electron density

Basically: $n_{up} / n_{lower} = \text{function}(T, n_e)$

Analytical radiative transfer: the Milne-Eddington atmosphere

- A simple analytical solution for a spectral line exists for a Milne-Eddington atmosphere (i.e. $\eta_0 = (\kappa_L / \kappa_C)$ independent of τ_C and S_L depending only linearly on τ_L).

$$I(\mu)/I_C(\mu) = \beta \mu / (1 + \eta_0),$$

$I(\mu)/I_C(\mu)$ = continuum-normalized emergent intensity, where $\eta_0 = (\kappa_L / \kappa_C)$ and β is derivative of Planck function with respect to τ_ν .

- The term $(1 + \eta_0)$ takes care of line saturation.
- As absorption due to line, η_0 , increases, $I(\mu)$ initially decreases, but for large η_0 saturates around 0.

Illustration of line saturation

- 4 spectral lines computed in Milne-Eddington atmospheres
- As η_0 increases the line initially becomes deeper, then wider, finally showing prominent line wings

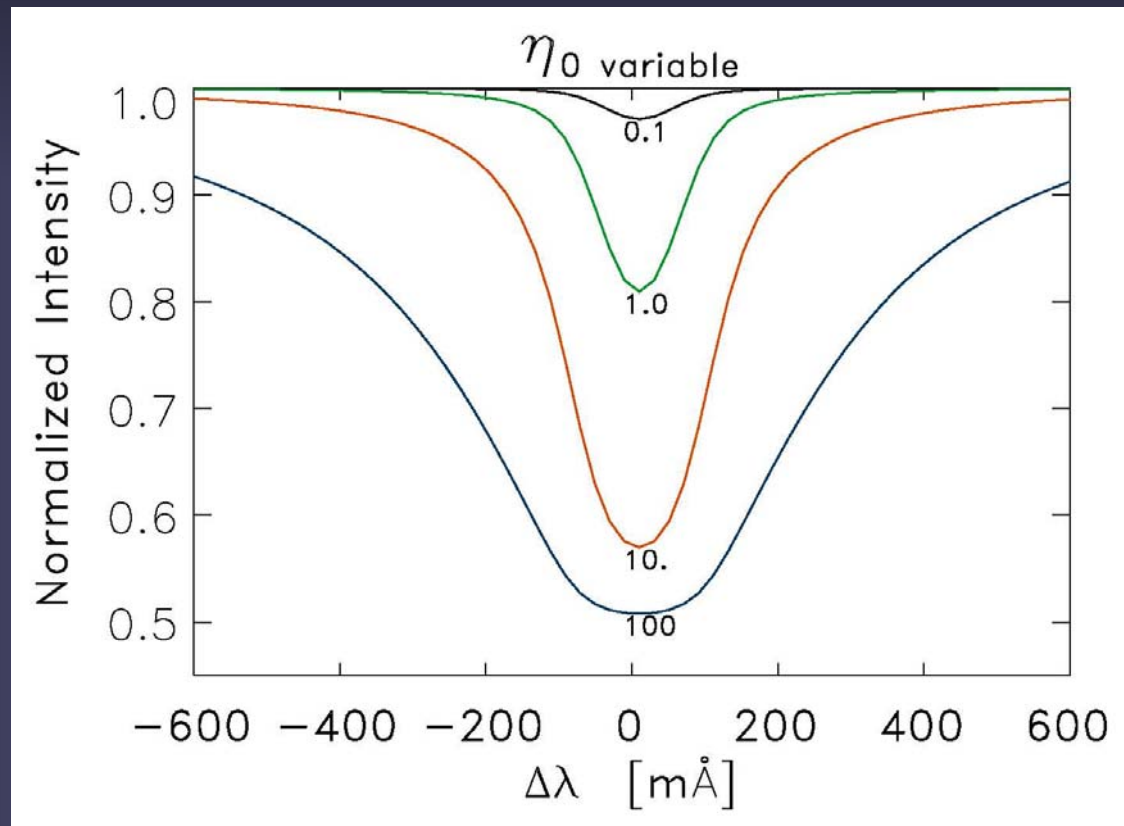
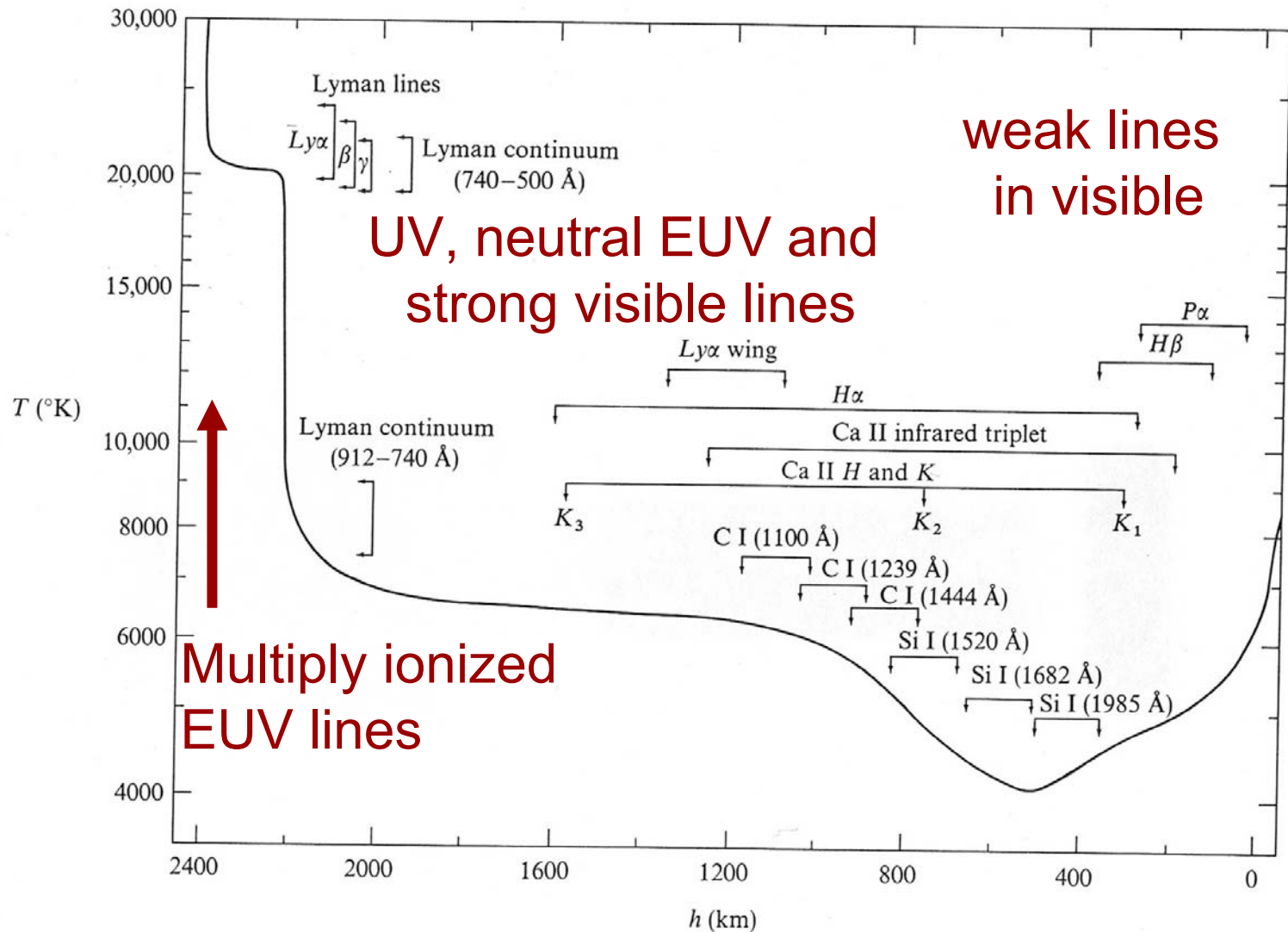


Figure kindly provide by J.M. Borrero

Diagnostic power of spectral lines

- Different parameters describing line strength and line shape contain information on different parameters of the solar/stellar atmosphere:
 - **Doppler shift of line:** (net) flows in the LOS direction.
 - **Line width:** temperature and turbulent velocity
 - **Equivalent width:** elemental abundance, temperature (via ionisation and excitation balance)
 - **Line depth:** temperature and temperature gradient
 - **Line asymmetry:** velocity gradients, v , T inhomogeneities
 - **Wings of strong lines:** gas pressure
 - **Polarisation and splitting:** magnetic field

Heights of formation: on which layers do lines give information ?



Solar convection

Hydrostatic equilibrium

- Sun is (nearly) hydrostatically stratified (this is the case even in the convection zone). I.e. gas satisfies:

$$dP/dz = -g\rho = -gP/\mu RT$$

(P pressure, g grav. accel., ρ density, μ mean molec. weight, R gas constant)

- Solution for constant temperature:

$$P = P_0 \exp(-z/H)$$

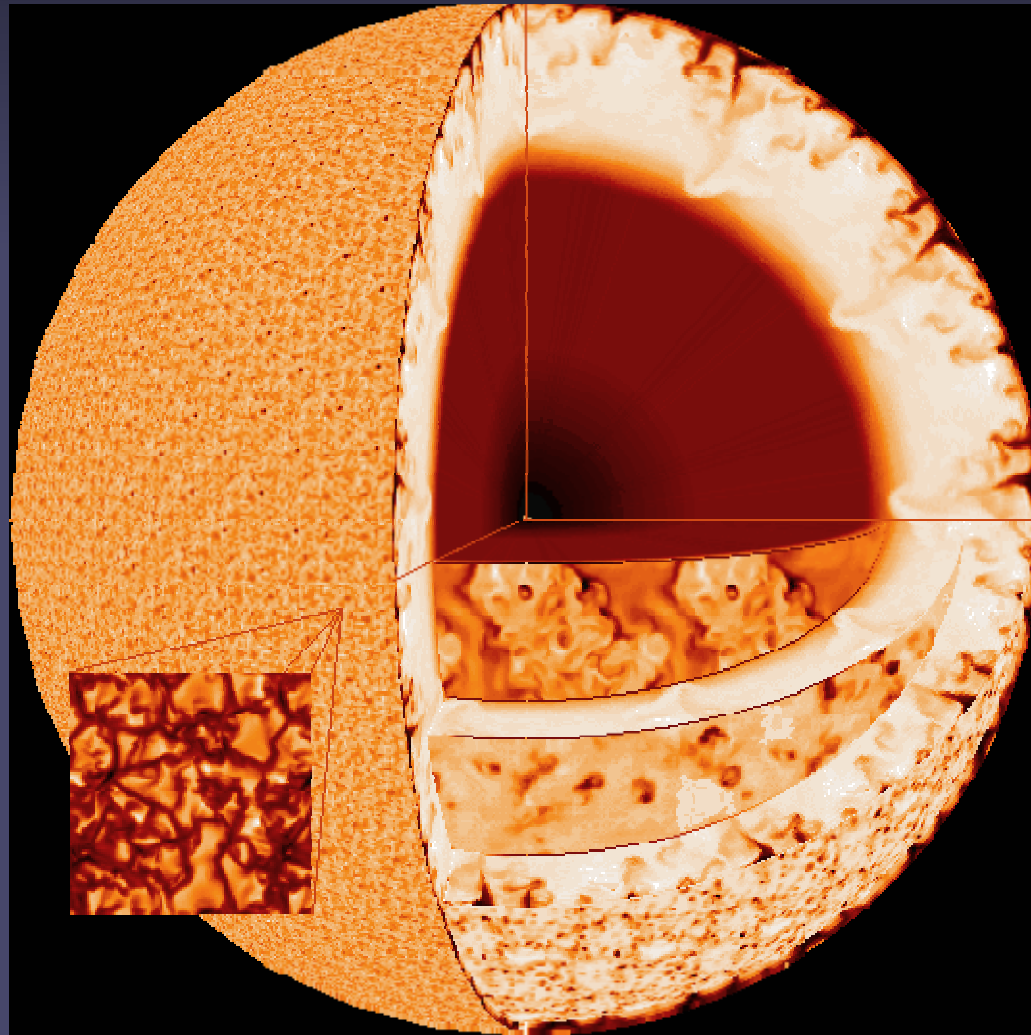
- Here H is the pressure scale height. $H \sim T^{1/2}$ and varies between 100 km in photosphere (solar surface) and 10^4 km at base of convection zone.

The convection zone

- Through the outermost 30% of solar interior, energy is transported by convection instead of by radiation
- In this layer the gas is convectively unstable.
- I.e. the process changes from a random walk of the photons through the radiative zone (due to high density, the mean free path in the core is well below a millimeter) to convective energy transport
- The unstable region ends just below the solar surface. I.e. the visible signs of convection are actually due to overshooting (see following slides)
- $t_{\text{radiative}} \sim 10^6 \text{ years} \gg t_{\text{convective}} \sim \text{days-weeks}$

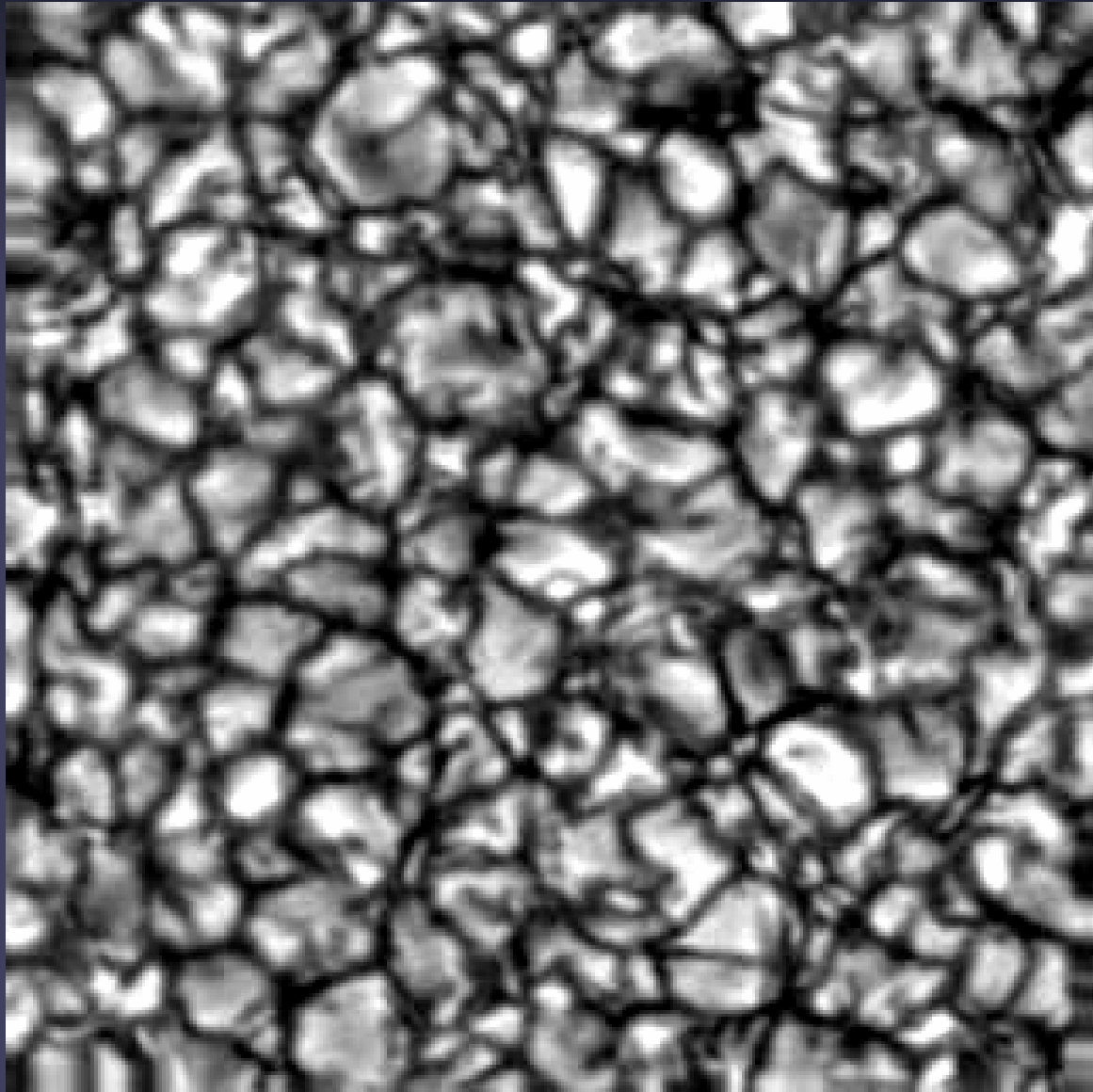
Scales of solar convection

- Observations: 4 main scales
 - granulation
 - mesogranulation
 - supergranulation
 - giant cells
- Colour:
 - well observed
 - less strong evidence
- Theory: larger scales at greater depths. Most details still unclear



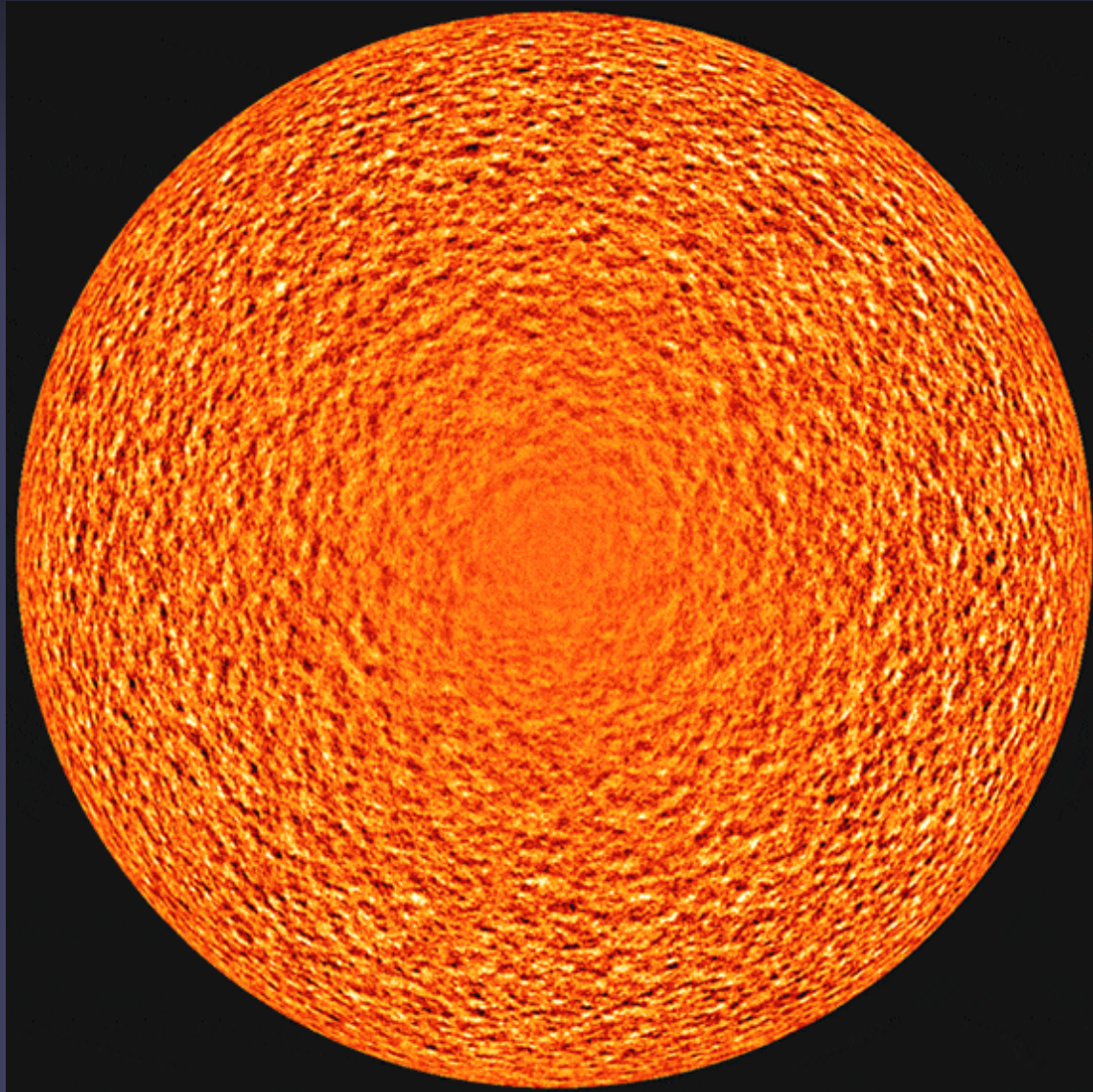
Surface manifestation of convection: granulation

- Typical size: 2 Mm
- Lifetime: 6-8 min
- Velocities: 1 km/s (but peak velocities > 10 km/s, i.e. supersonic)
- Brightness contrast: 15% in visible(yellow) continuum (under ideal conditions)
- All quantities show a continuous distribution of values
- At any one time 10^6 granules on sun.



Surface manifestation of convection: Supergranulation

- 1 hour average of MDI Dopplergrams (averages out oscillations).
- Dark-bright: flows towards/away from observer.
- No supergranules visible at disk centre: velocity is mainly horizontal
- **Size:** 20-30 Mm, **lifetime:** days, **horiz. speed:** 400 m/s, **no contrast** in visible



Observing convection

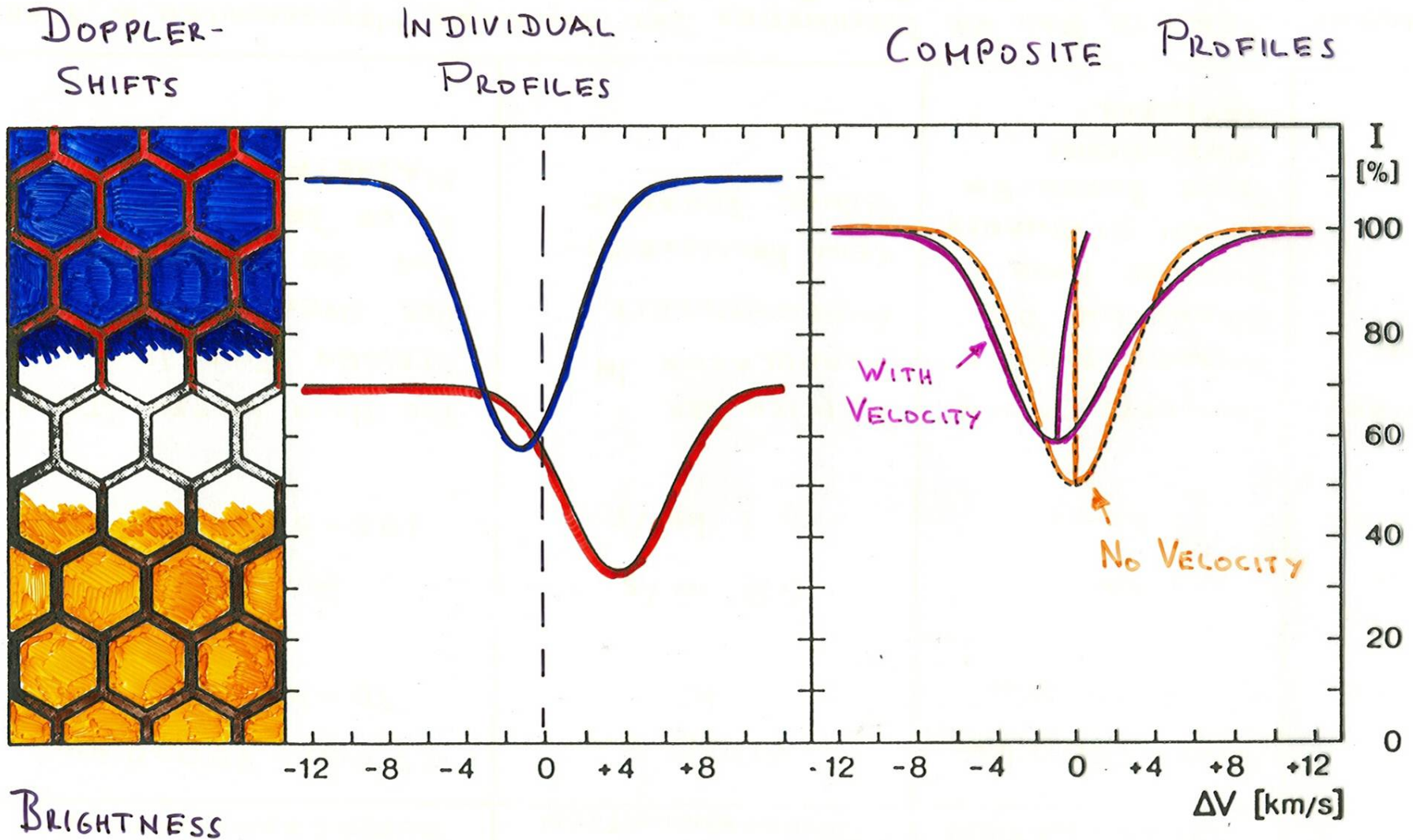
■ Observing granulation

- Continuum images and movies at high spatial resolution: gives sizes, lifetimes and evolution (splitting and dissolving granules), contrasts
- Spectral lines. Line bisectors, line widths and convective blue shifts: contrasts, area factors, stratification

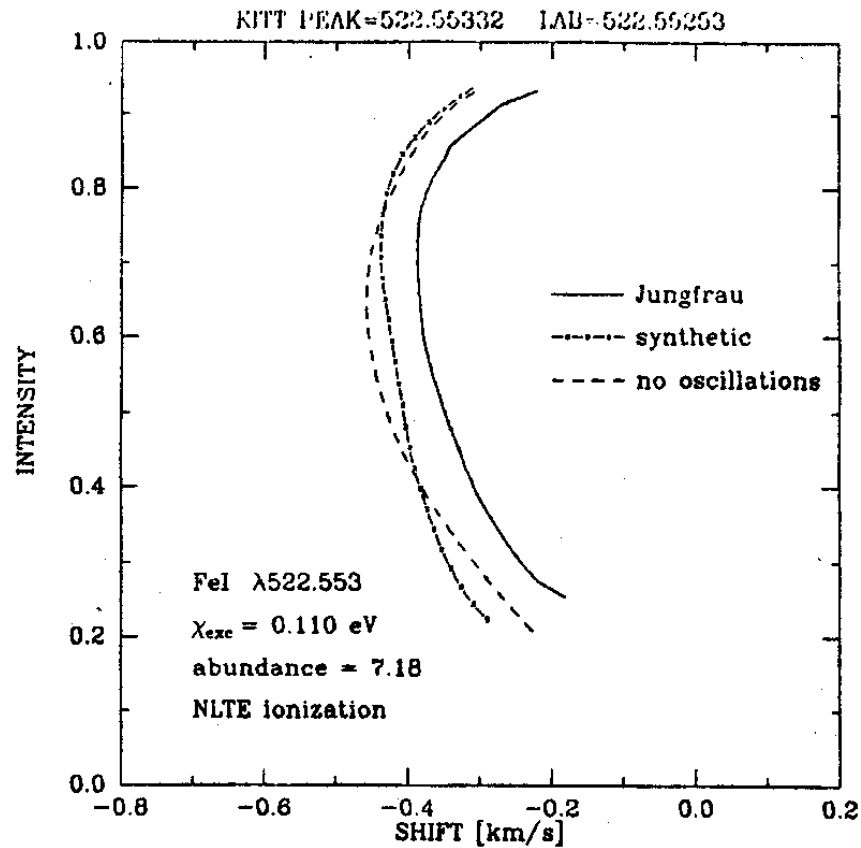
■ Observing supergranulation

- Images and movies in cores of chromospheric spectral lines, or magnetograms: observe the magnetic field at the edges of the supergranules instead of the supergranules directly
- Helioseismic techniques

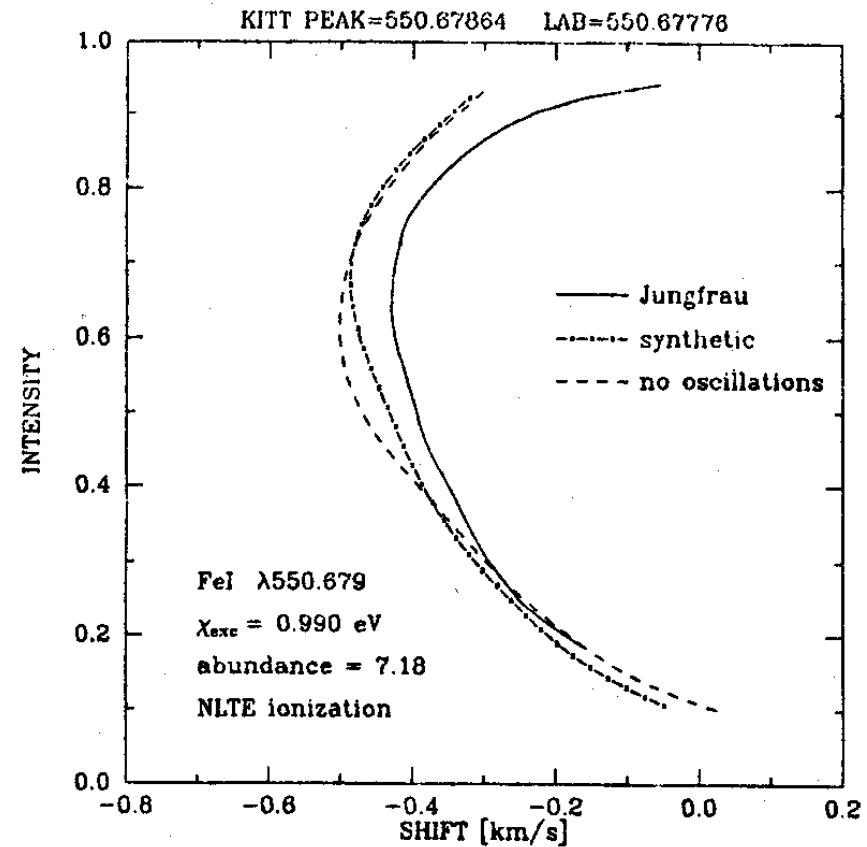
Line bisectors



Observed line bisectors: "C" shape

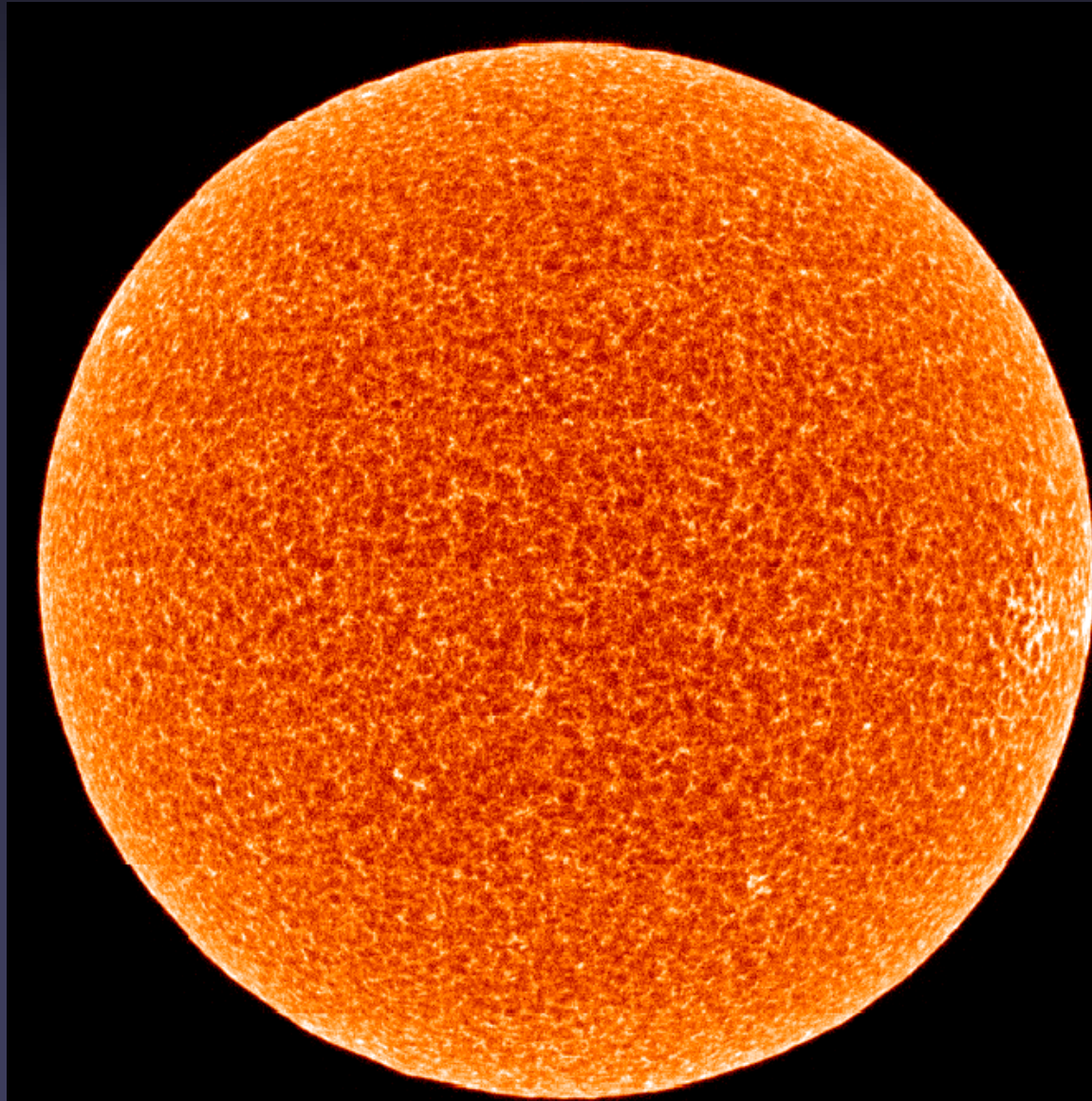


C.



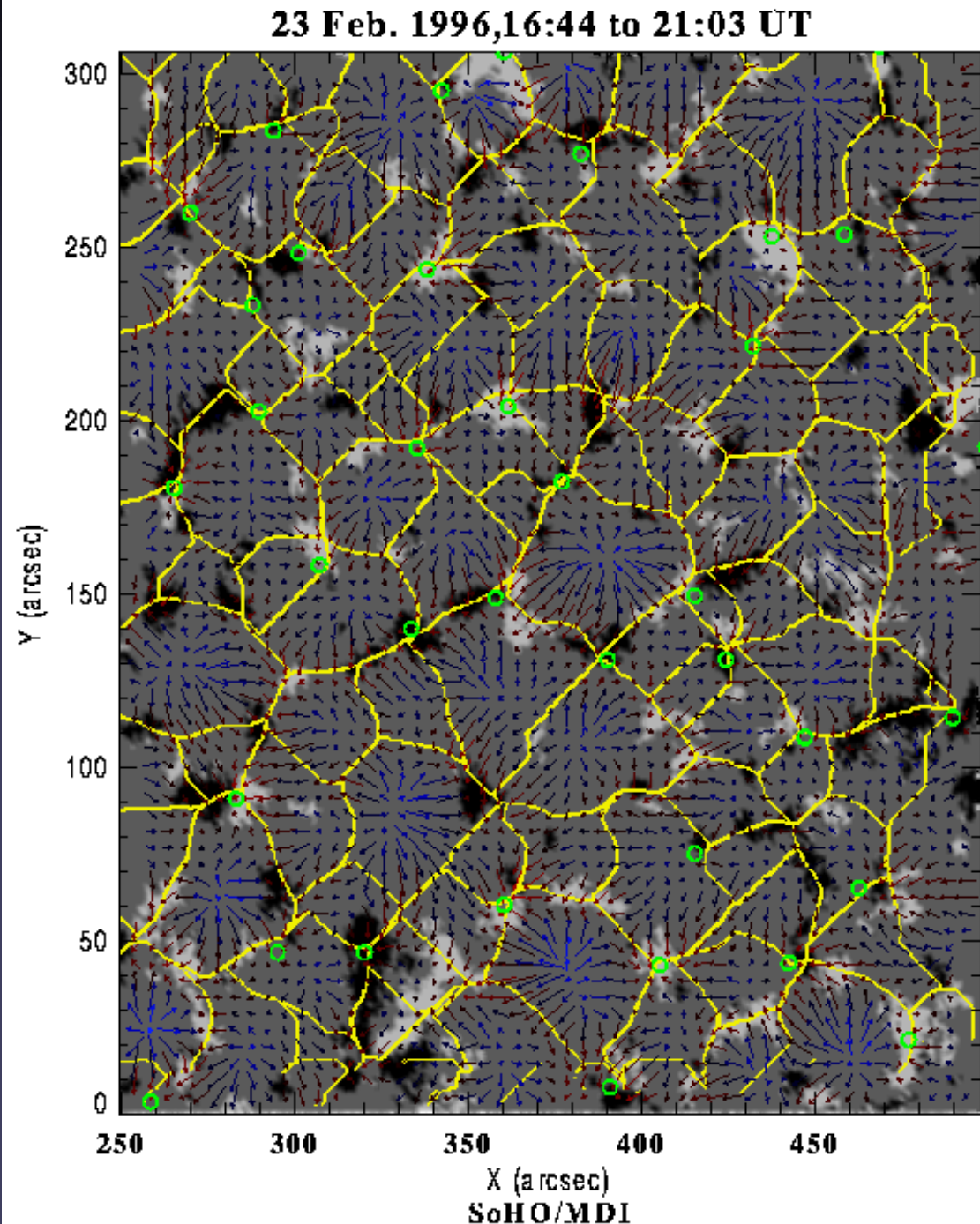
Supergranules seen by SUMER

- Si I 1256 Å full disk scan by SUMER in 1996
- Bright network indicates location of magnetic network
- Darker cells: supergranules



Supergranules & magnetic field

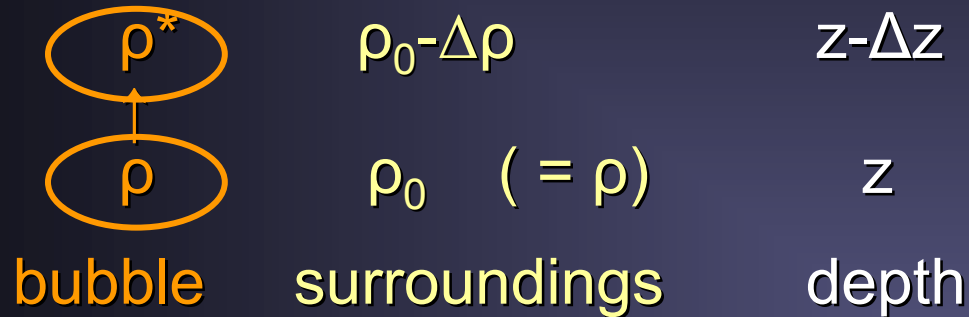
- Why are supergranules seen in chromospheric and transition region lines?
- Supergranules are related to the magnetic network.
- Network magnetic fields are located at edges of supergranules. They appear bright in UV.



Onset of convection

Schwarzschild's instability criterion

Consider a rising bubble of gas:



Condition for convective instability: $\rho^* < \rho_0 - \Delta\rho$

For small Δz , bubble will not have time to exchange heat with surroundings: adiabatic behaviour. Convectively unstable if:

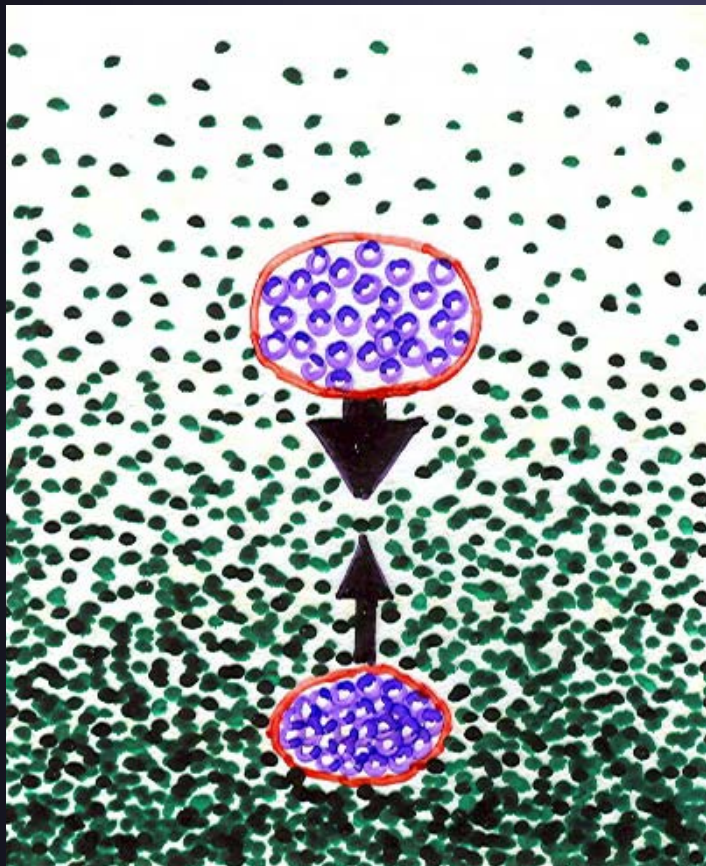
$$[dp/dz - (dp/dz)_{\text{adiab}}] \Delta z < 0$$

dp/dz : stellar density gradient if in radiative equilibrium

$(dp/dz)_{\text{adiab}}$: adiabatic gradient

Illustration of convectively stable and unstable situations

Convectively **stable**



Convectively **unstable**



Onset of convection II

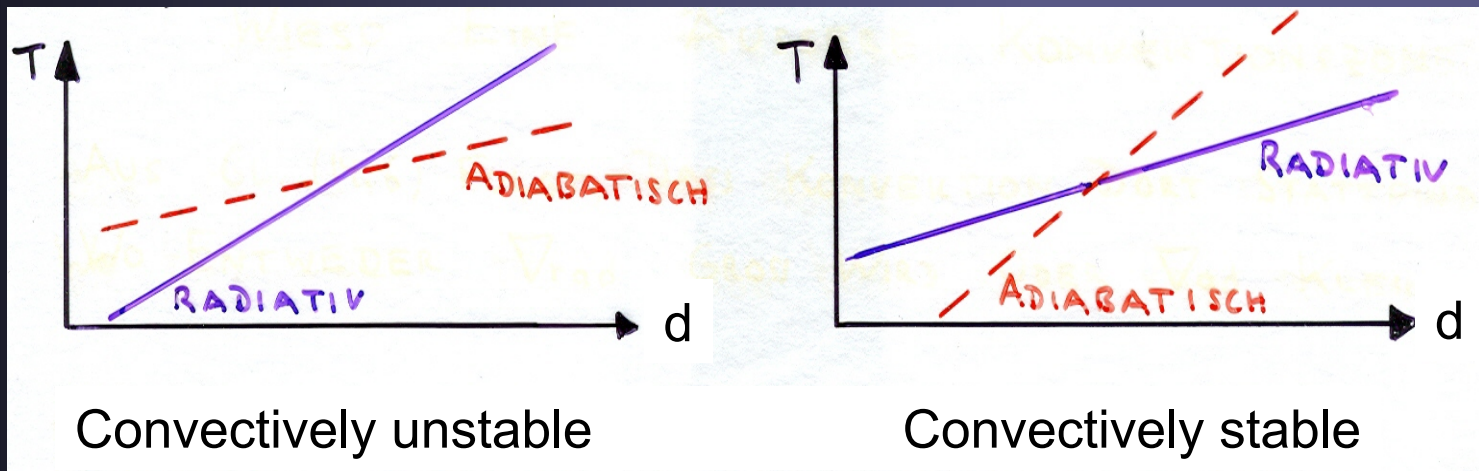
Rewriting in terms of temperature and pressure:

$$\nabla_{\text{ad}} = (d \log T / d \log P)_{\text{ad}}$$

$\nabla_{\text{rad}} = (d \log T / d \log P)_{\text{rad}} =$ gradient in an atmosphere with radiative energy transport

Schwarzschild's convective instability criterion:

$$\nabla_{\text{ad}} < \nabla_{\text{rad}}$$



Why an outer convection zone?

- Why does radiative grad exceed adiabatic gradient?
- Mainly: radiative gradient becomes very large due to ionization of H and He below the solar surface.
- Expression for radiative gradient (for Eddington approximation):

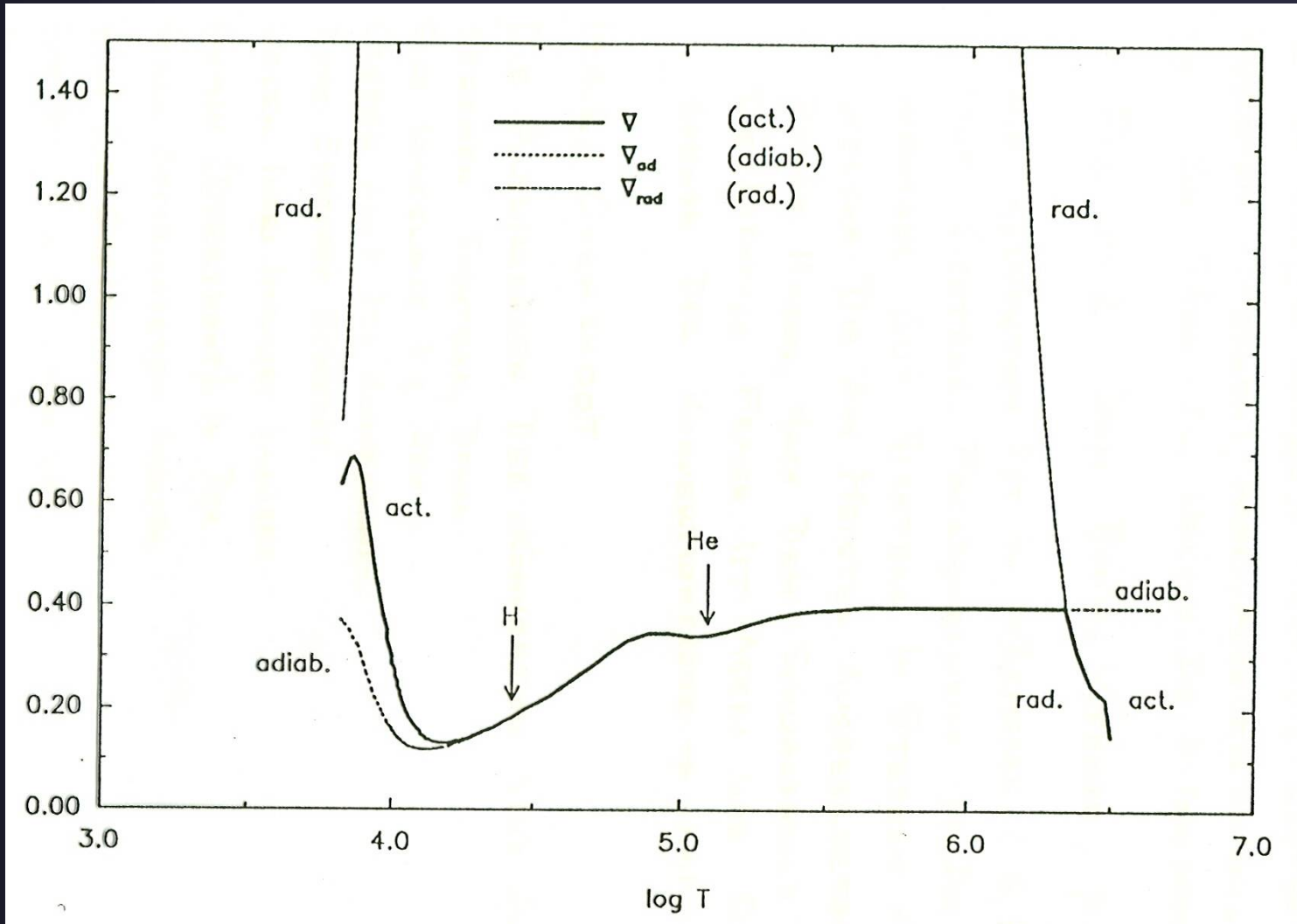
$$\nabla_{\text{rad}} = (3F_r / 16\sigma g) (\kappa_{\text{gr}} P_g / T^4)$$

- F_r = radiative flux (\approx constant)
- σ = Stefan-Boltzmann constant
- g = gravitational acceleration (\approx constant)
- κ_{gr} = absorption coefficient per gram. At surface H and He are neutral. They become ionized with depth as T grows
→ κ_{gr} increases rapidly, leading to large radiative gradient.

Ionisation of H and He

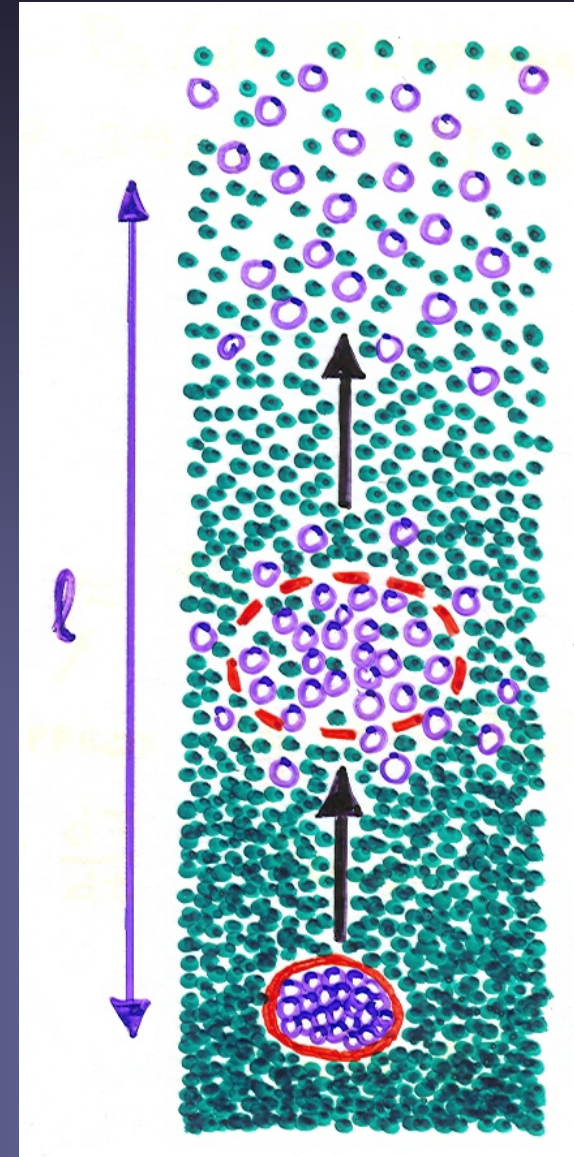
- Ionisation balance is described by Saha's equation: degree of ionisation depends on T and n_e
- H ionisation happens just below solar surface
- $\text{He} \rightarrow \text{He}^+ + e^-$ happens 7000 km below surface
- $\text{He}^+ \rightarrow \text{He}^{++} + e^-$ happens 30'000 km below surface
- Since H is most abundant, it provides most electrons (largest opacity) and drives convection most strongly
- At still greater depth, ionization of other elements also provides a minor contribution.

Radiative, adiabatic & actual gradients



The mixing length

- As a gas packet rises, diffusion of particles and thermal exchange with surroundings causes it to lose its identity and to stop moving on.
- Length travelled up to that point: mixing length l (from L. Prandtl)
- Often used parameterization of l :
$$l = \alpha H_p$$
 - H_p = pressure scale height
 - α = mixing length parameter, typically 1-2 (determined empirically)



Convective overshoot

- Due to their inertia, the packets of gas reaching the boundary of the CZ pass into the convectively stable layers, where they are braked & finally stopped.
- overshooting convection
- Typical width of overshoot layer: order of H_p
- This happens at both the bottom and top boundaries of the CZ and is important:
 - top boundary: Granulation is overshooting material. $H_p \approx 100$ km in photosphere
 - bottom boundary: the overshoot layer allows B-field to be stored → seat of the dynamo?

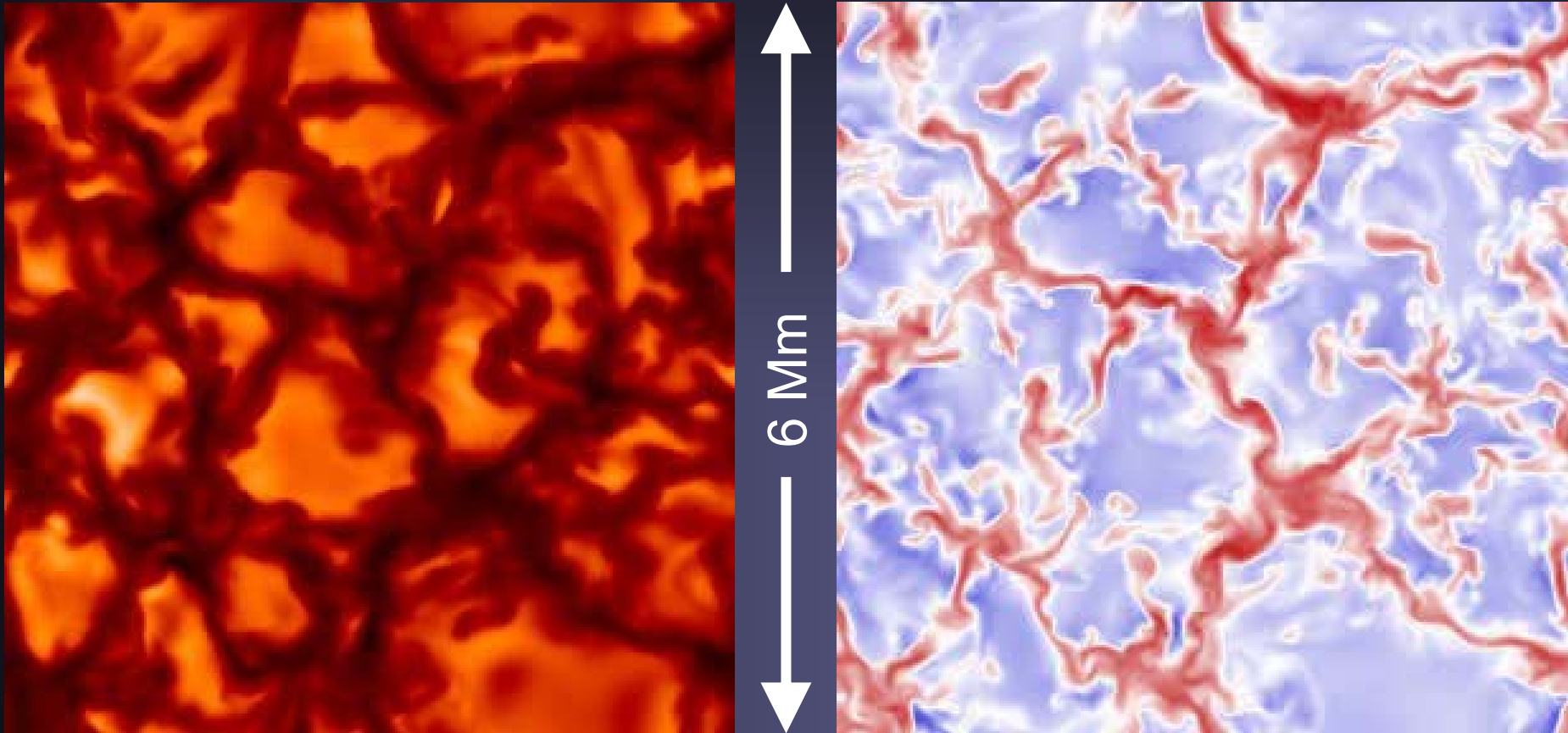
Convection simulations

- 3-D hydrodynamic simulations reproduce a number of observations and provide new insights into solar convection.
- These codes solve for mass conservation, momentum conservation (force balance, Navier-Stokes equation), and energy conservation including as many terms as feasible.
- Problem: Simulations can only cover 2-3 orders of magnitude in length scale (due to limitations in computing power), while the physical processes on the Sun act over at least 6 orders of magnitude.
- Also, simulations can only cover a part of the size scale of solar convection, either granulation, supergranulation, or larger scales, but not all.

Convection simulations II

- Simulations do not achieve the solar Reynolds number ($R_e = vl/\nu$) of 10^{10} , where v = typical velocity, l = typical length scale, ν = kinematic viscosity ($R_e \sim$ ratio of viscous to advection time scales).
- For comparison with observations it is important that the simulations describe the surface layers well, i.e. code needs to consider:
 - radiative transport of energy. Only few simulation codes do this properly.
 - partial ionization of many elements
 - as low a viscosity as numerically possible
- The role of radiation is primarily to transport energy. At the solar surface the energy transported by radiation becomes comparable to that by convection.

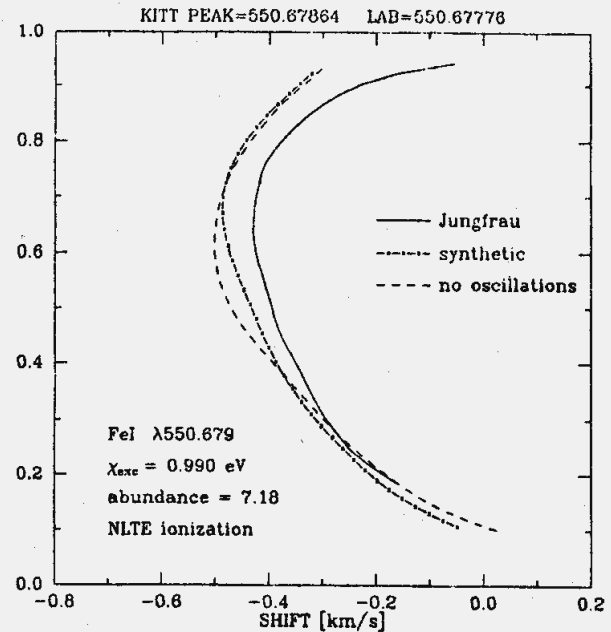
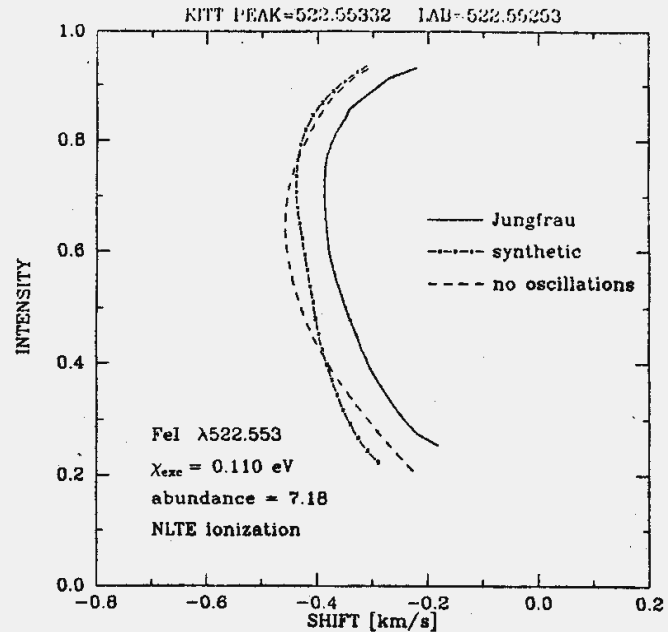
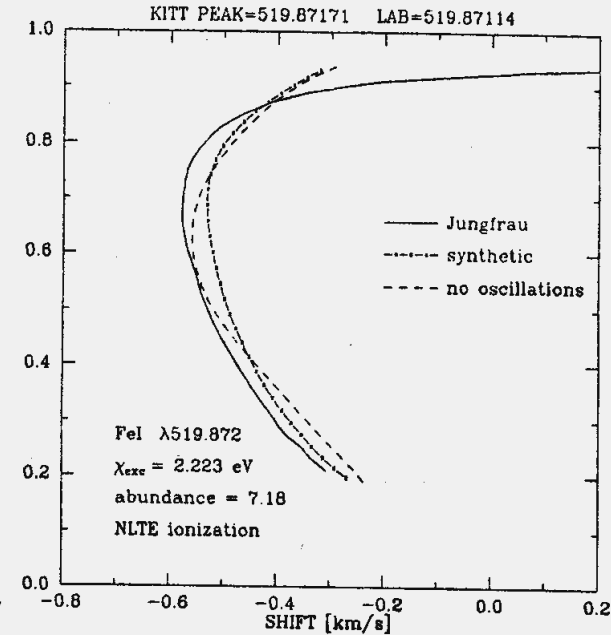
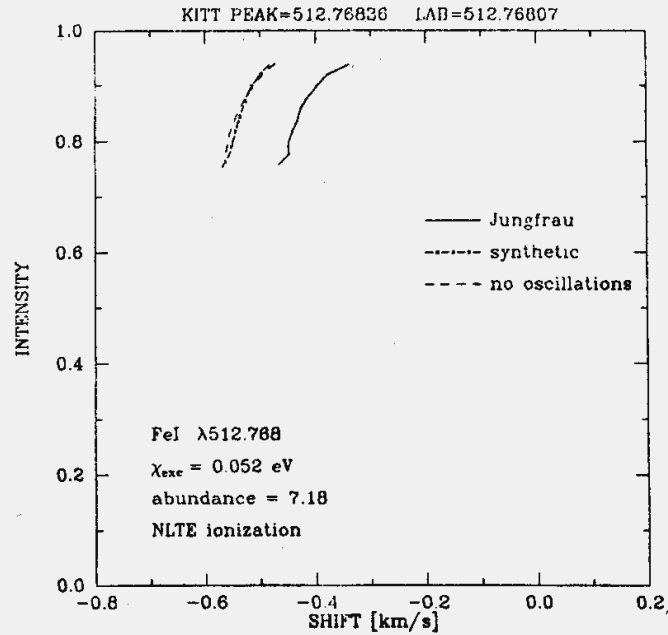
Simulations of solar granulation



Solution of Navier-Stokes equation etc. describing fluid dynamics in a box (6000 km x 6000 km x 1400 km) containing the solar surface. Realistic looking granulation is formed.

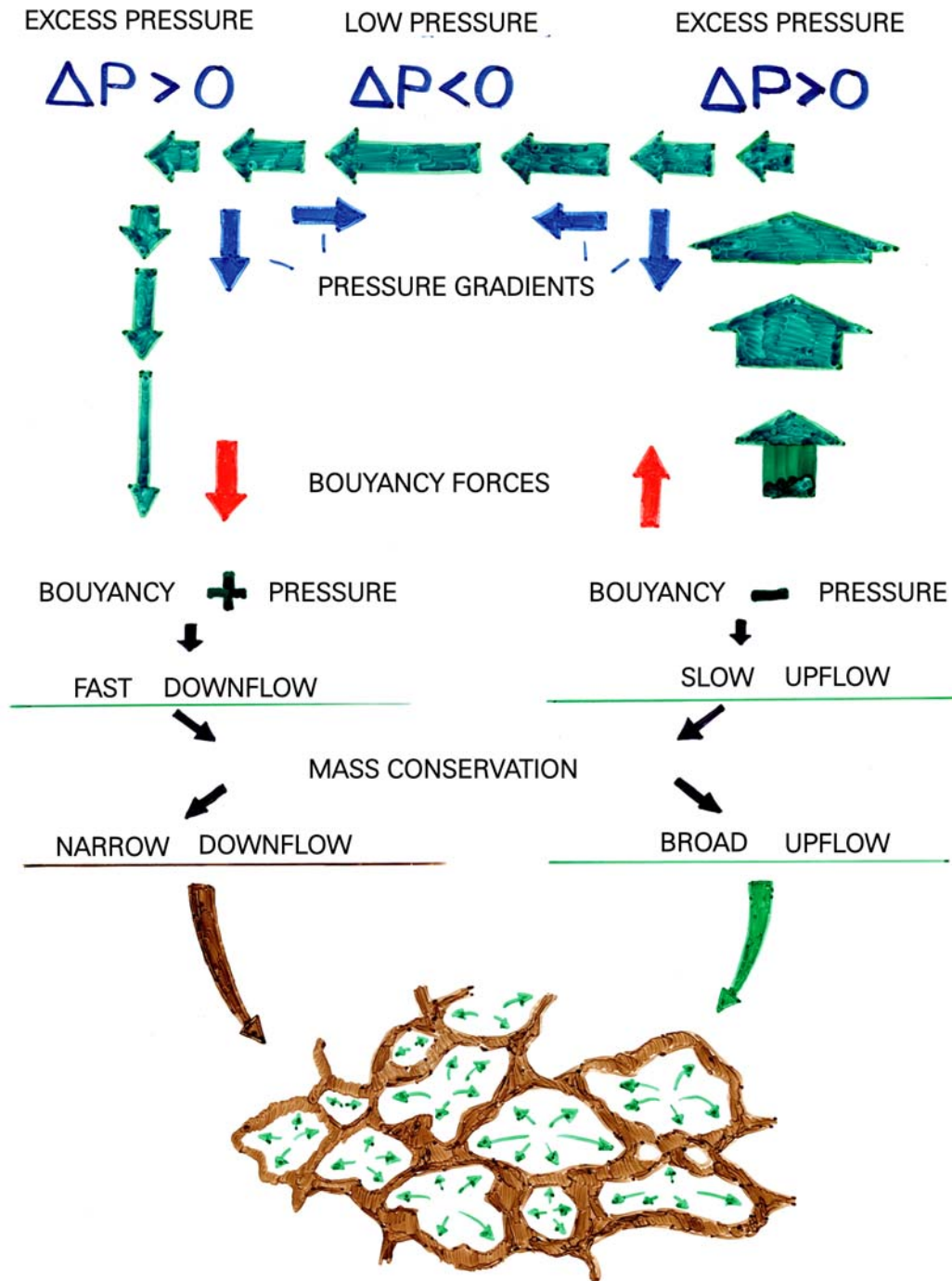
Testing the simulations

Comparison between observed and computed bisectors for selected spectral lines (2 computed bisectors shown: one each with and without oscillations in the atmosphere)



Granule structure

Upflows are broad & slow, downflows are narrow and fast.
Why?



Granule evolution

- Granules die in two ways:
 - **dissolve**: grow fainter and smaller until they disappear (small granules)
 - **split**: break into two smaller granules (large granules)
- Granules are born in two ways:
 - as fragments of a large splitting granule
 - appearing as small structures and growing
- Initially most granules grow in size, some keep growing until they become unstable (see next slide) and split, others stop growing and start shrinking until they disappear (all within 5-10 min).

Relation between granules and supergranules

- Downflows of granules continue to bottom of simulations, but the intergranular lanes break up into isolated narrow downflow plumes.
- I.e. topology of flow reverses with depth:
 - At surface: isolated upflows, connected downflows
 - At depth: connected upflows, isolated downflows
- Idea put forward by Spruit et al. 1990: At increasingly greater depth the narrow downflows from different granules merge, forming a larger and less fine-meshed network that outlines the supergranules

Increasing size of convective cells with depth

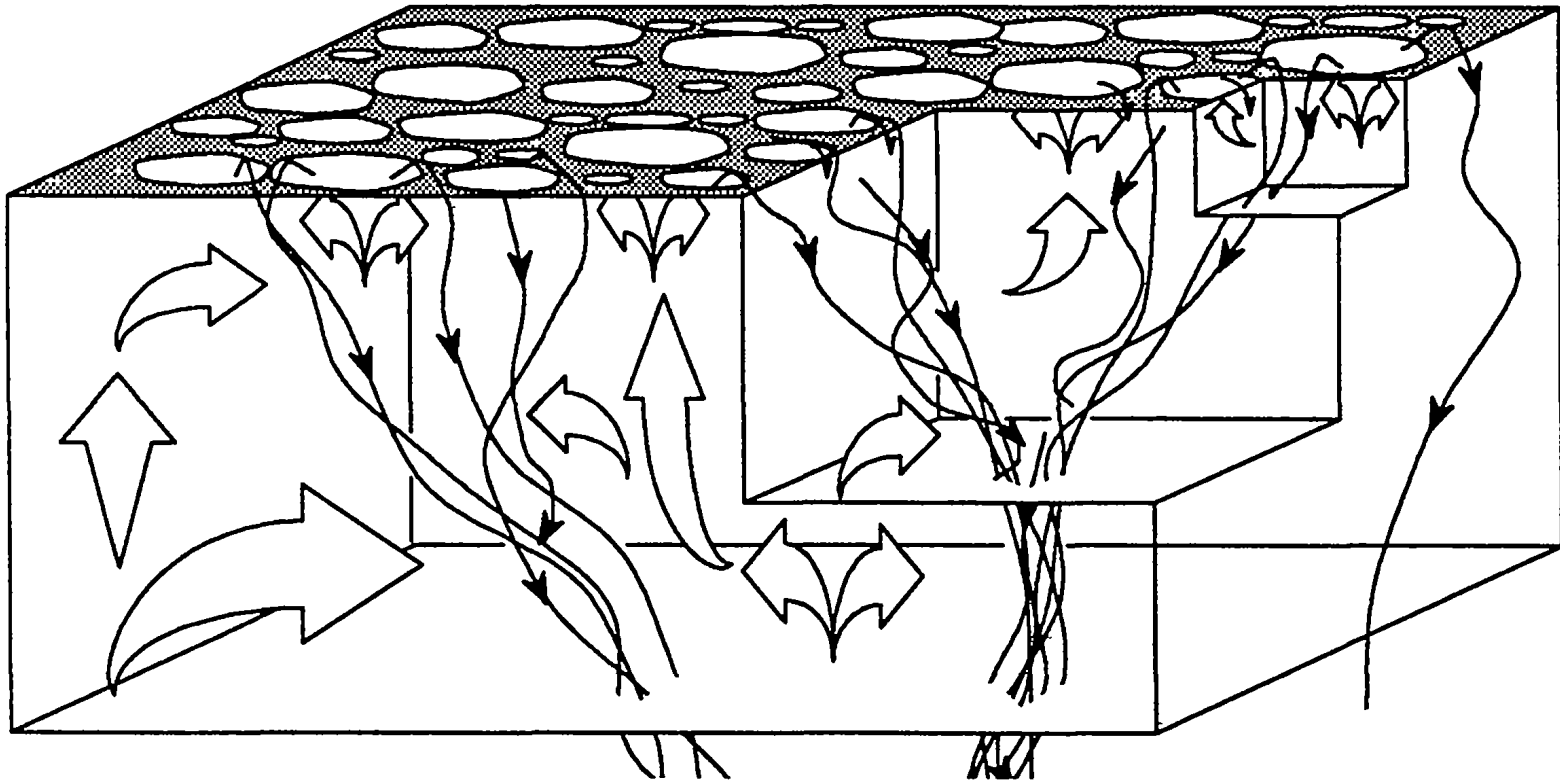


Figure 7 Flow lines showing the merging of the downdrafts on successively larger scales (schematic). The boxes cut out illustrate how the same process occurs on (in this illustration) three different scales.

Convection on other stars

- F, G, K & M stars (& cool WDs) possess outer convection zones
- Observations are difficult since surfaces cannot be resolved.
→ Use line bisectors
- A, F stars show inverse bisectors: granulation has different geometry.
- Hot stars have an inner convection zone

